stress affects BDNF level in the hippocampus, hypothalamus and pituitary, and BDNF may play a "protective" role during stress *via* regulation of HPA axis [12–14]. In fact, direct infusion of BDNF into midbrain or hippocampus can reduce the immobility time in depression-like rats [11,17].

BDNF induces cell survival, proliferation and differentiation *via* activation of the signaling pathway downstream of TrkB [6,7,45]. We examined the phosphorylation of Akt, p44/42 MAPK, S6K and S6, which act downstream of the BDNF/TrkB signaling pathway. We found that phosphorylation levels of these factors were higher in the Leu–Ile-treated group than in those of the vehicle-treated group under conditions of repeated FST (Fig. 2). These results suggest that Leu–Ile activates the Akt/mTOR pathway downstream of BDNF. Moreover, treatment with the mTOR inhibitor, rapamycin, reduced BDNF induction by Leu–Ile (Fig. 3B). These results suggest that activation of the Akt/mTOR pathway is necessary for BDNF induction by Leu–Ile. Akt activation increases the phosphorylation of CREB followed by BDNF induction. mTOR signaling pathway may support the Akt activation *via* phosphorylation of Ser473 of Akt [46].

FST is used as means for testing the antidepressant-like effects of new therapeutic tools or medicines [25,26]. The shortening of length of immobility time during swimming for 6 min is an indicator of the antidepression-like effect. In the present study, daily repeated FST for 2 weeks prolonged immobility time (Fig. 4C). Interestingly, repeated Leu–Ile administration reduced the prolongation of immobility time after 2 weeks (Fig. 4C). Since repeated Leu–Ile did not affect spontaneous motor activity in non-FST mice (Supplement data 1), the Leu–Ile-mediated reduction in immobility time was not due to an increase of spontaneous motor activity.

Typical or classical antidepressants, for example tricyclics and serotonin reuptake inhibitors (SSRI), reduce the immobility time of FST with one shot treatment, because these drugs show the effect by inhibition of the monoamine re-uptake and increase concentration of serotonin or noradrenaline. The SSRI also increase the BDNF induction by repeated administration and the BDNF induction is important for the anti-depressant effects [18,19,47]. The SSRI also increase cell proliferation in dentate gyrus with long repeated treatment in rat [31,48,49]. Moreover, both of SSRI [27] and Leu–Ile ameliorate the cell proliferation in the hippocampus of repeated FST treatment mice (Fig. 7). These results suggested that Leu–Ile has an anti-depressant like effect as same as typical anti-depressants. Then the investigation of Leu–Ile needs 2 weeks for the effects of anti-depressant.

To confirm the requirement of BDNF for the antidepressant-like effect of Leu–Ile, we used BDNF(+/−) mice. These mice have half the level of hippocampal BDNF mRNA compared to BDNF(+/+) mice (Fig. 4B). BDNF(+/−) mice received the same treatment and behavioral test as BDNF(+/+) mice (Fig. 4A). In the FST, the immobility time following repeated Leu–Ile-treatment in BDNF(+/−) mice was not different from that of vehicle-treated mice (Fig. 4D). Furthermore, BDNF mRNA levels in the hippocampus of Leu–Ile-treated BDNF(+/−) mice were the same as those of vehicle-treated mice (Fig. 4B). In the case of the imipramine-treated BDNF(+/−) mice, the immobility time was not significantly different from that of the vehicle-treated (BDNF(+/+) or BDNF(+/−)) mice [50]. These results suggest that the antidepressant-like effect of Leu–Ile depends on BDNF expression.

Since *p.o.* administration is more convenient than *s.c.* in the clinical context, we also evaluated the effect of Leu–Ile (*p.o.*). The optimal dose of Leu–Ile for *p.o.* administration was 750 μmol/kg (Fig. 5B). The dose–response relationship for Leu–Ile showed a bell shaped pattern (Fig. 5B). This pattern is supported by our previous data that Leu–Ile induced glial cell line-derived neurotrophic factor and tumor necrosis factor-α with a bell-shaped dose–response relationship [24]. Since orally administrated Leu–Ile (750 μmol/kg) also reduced the prolongation of immobility time induced by repeated FST (Fig. 6B), Leu–Ile is suggested to be an antidepressant tool for oral administration.

Meta-analysis of volumetric studies has demonstrated that hippocampal volume is decreased in depressed patients [1]. Moreover, blocking hippocampal neurogenesis is sufficient to increase HPA axis activity, which highly related with depressive disorder [4]. The mechanism of reduction of hippocampal volume is not clear. However, neuronal degeneration and inhibition of cell proliferation in the dentate gyrus are considered to be contributory factors in this reduction, because this area is a site of major cell proliferation in the adult hippocampus. The adult mammalian brain, especially the dentate gyrus of the hippocampus, contains neural stem cells which provide new neurons [51]. Chronic stress causes shortening and debranching of dendrites in the CA3 region of the hippocampus and suppresses neurogenesis in the dentate gyrus [52]. BDNF has important roles in the neurogenesis [8,9,53,54], and also in the reduction of the depression-like behavior [41]. It is not clear how effect of BDNF is on the recovery of cell proliferation in the dentate gyrus, since *in vivo* study, BDNF-knock down in the dentate gyrus by RNA interference and lentiviral vectors does not have effect on the cell proliferation but reduced neuronal differentiation [9]. Although repeated FST for 3 weeks reduces cell proliferation in the dentate gyrus of mice, antidepressant drugs reverse this reduction [27]. We therefore examined the effect of Leu–Ile on cell proliferation in the dentate gyrus, using BrdU labeling of proliferating cells. Repeated FST for 2 weeks reduced numbers of BrdU positive cells in the dentate gyrus (Fig. 7B, D and F). Leu–Ile administration after daily FST recovered BrdU positive cell numbers in mice undergoing repeated FST (Fig. 7D–F), but had no such effect in mice not undergoing FST. It is interesting that Leu–Ile affected only brains damaged by FST. Leu–Ile administration also did not affect BDNF mRNA levels in mice that did not undergo FST (data not shown). It is likely that Leu–Ile is an enhancer rather than an initiator of the cellular protective system in the damaged brain. Leu–Ile may enhance expression of BDNF induced by another trigger under stressful conditions. For example, stress is one of the triggers of BDNF induction in the hippocampus, hypothalamus and pituitary, and BDNF may play a "protective" role during stress *via* regulation of HPA axis [12–14,55,56]. In the present data, Leu–Ile may support the regulation of HPA axis during stress *via* increase of BDNF mRNA level in the hippocampus.

There is a question as to whether Leu–Ile enters the brain and produces an antidepressant-like effect. It is likely that Leu–Ile itself affects the brain directly, since *i.c.v.*-injection of Leu–Ile increases BDNF in mouse striatum [23]. Moreover, repeated administration of a mixture of Leu and Ile did not affect the prolongation of immobility time induced by repeated FST (Fig. 8B). It has not yet been possible to detect Leu–Ile in the brain, but the existence of a dipeptide transporter in the brain suggests the possibility of dipeptide uptake [57].

Our present results indicate that Leu–Ile is a therapeutic tool, acting *via* BDNF induction, for depression. Moreover, Leu–Ile may safe to use for long-term treatment for depression, since this dipeptide is present in foods [58]. Furthermore, Leu–Ile does not have an immunosuppressive effect, although its structure resembles a partial structure of FK506. On the other hand, BDNF is a key contributory factor not only in depression, but also other psychoses, since the BDNF Val66Met allele is implicated in a variety of psychiatric diseases [59,60]. Therefore, BDNF inducers, including Leu–Ile, could be useful therapeutic tools for various psychiatric disorders.

Appendix A. Supplementary data

Supplementary data associated with this article can be found, in the online version, at doi:10.1016/j.bbr.2011.02.003.

References

[1] Campbell S, Marriott M, Nahmias C, MacQueen GM. Lower hippocampal volume in patients suffering from depression: a meta-analysis. Am J Psychiatry 2004;161:598–607.
[2] Gould E, Tanapat P. Stress and hippocampal neurogenesis. Biol Psychiatry 1999;46:1472–9.
[3] Santarelli L, Saxe M, Gross C, Surget A, Battaglia F, Dulawa S, et al. Requirement of hippocampal neurogenesis for the behavioral effects of antidepressants. Science 2003;301:805–9.
[4] Schloesser RJ, Manji HK, Martinowich K. Suppression of adult neurogenesis leads to an increased hypothalamo-pituitary-adrenal axis response. Neuroreport 2009;20:553–7.
[5] Sweatt JD. The neuronal MAP kinase cascade: a biochemical signal integration system subserving synaptic plasticity and memory. J Neurochem 2001;76:1–10.
[6] Encinas M, Iglesias M, Llecha N, Comella JX. Extracellular-regulated kinases and phosphatidylinositol 3-kinase are involved in brain-derived neurotrophic factor-mediated survival and neuritogenesis of the neuroblastoma cell line SH-SY5Y. J Neurochem 1999;73:1409–21.
[7] Takei N, Kawamura M, Hara K, Yonezawa K, Nawa H. Brain-derived neurotrophic factor enhances neuronal translation by activating multiple initiation processes: comparison with the effects of insulin. J Biol Chem 2001;276:42818–25.
[8] Pencea V, Bingaman KD, Wiegand SJ, Luskin MB. Infusion of brain-derived neurotrophic factor into the lateral ventricle of the adult rat leads to new neurons in the parenchyma of the striatum, septum, thalamus, and hypothalamus. J Neurosci 2001;21:6706–17.
[9] Taliaz D, Stall N, Dar DE, Zangen A. Knockdown of brain-derived neurotrophic factor in specific brain sites precipitates behaviors associated with depression and reduces neurogenesis. Mol Psychiatry 2010;15: 80–92.
[10] Kohara K, Yasuda H, Huang Y, Adachi N, Sohya K, Tsumoto T. A local reduction in cortical GABAergic synapses after a loss of endogenous brain-derived neurotrophic factor, as revealed by single-cell gene knock-out method. J Neurosci 2007;27:7234–44.
[11] Luscher B, Shen Q, Sahir N. The GABAergic deficit hypothesis of major depressive disorder. Mol Psychiatry 2010 (in press).
[12] Givalois L, Naert G, Rage F, Ixart G, Arancibia S, Tapia-Arancibia L. A single brain-derived neurotrophic factor injection modifies hypothalamo-pituitary-adrenocortical axis activity in adult male rats. Mol Cell Neurosci 2004;27:280–95.
[13] Naert G, Ixart G, Tapia-Arancibia L, Givalois L. Continuous i.c.v. infusion of brain-derived neurotrophic factor modifies hypothalamic–pituitary–adrenal axis activity, locomotor activity and body temperature rhythms in adult male rats. Neuroscience 2006;139:779–89.
[14] Kunugi H, Hori H, Adachi N, Numakawa T. Interface between hypothalamic–pituitary–adrenal axis and brain-derived neurotrophic factor in depression. Psychiatry Clin Neurosci 2010;64:447–59.
[15] Molendijk ML, Bus BA, Spinhoven P, Penninx BW, Kenis G, Prickaerts J, et al. Serum levels of brain-derived neurotrophic factor in major depressive disorder: state-trait issues, clinical features and pharmacological treatment. Mol Psychiatry 2010 (In press).
[16] Siuciak JA, Lewis DR, Wiegand SJ, Lindsay RM. Antidepressant-like effect of brain-derived neurotrophic factor (BDNF). Pharmacol Biochem Behav 1997;56:131–7.
[17] Shirayama Y, Chen AC, Nakagawa S, Russell DS, Duman RS. Brain-derived neurotrophic factor produces antidepressant effects in behavioral models of depression. J Neurosci 2002;22:3251–61.
[18] Nibuya M, Morinobu S, Duman RS. Regulation of BDNF and trkB mRNA in rat brain by chronic electroconvulsive seizure and antidepressant drug treatments. J Neurosci 1995;15:7539–47.
[19] Chen B, Dowlatshahi D, MacQueen GM, Wang JF, Young LT. Increased hippocampal BDNF immunoreactivity in subjects treated with antidepressant medication. Biol Psychiatry 2001;50:260–5.
[20] Butcher SP, Henshall DC, Teramura Y, Iwasaki K, Sharkey J. Neuroprotective actions of FK506 in experimental stroke: in vivo evidence against an antiexcitotoxic mechanism. J Neurosci 1997;17:6939–46.
[21] Zawadzka M, Kaminska B. Immunosuppressant FK506 affects multiple signaling pathways and modulates gene expression in astrocytes. Mol Cell Neurosci 2003;22:202–9.
[22] Tanaka K, Fujita N, Yoshioka M, Ogawa N. Immunosuppressive and non-immunosuppressive immunophilin ligands improve H(2)O(2)-induced cell damage by increasing glutathione levels in NG108-15 cells. Brain Res 2001;889:225–8.
[23] Nitta A, Nishioka H, Fukumitsu H, Furukawa Y, Sugiura H, Shen L, et al. Hydrophobic dipeptide Leu–Ile protects against neuronal death by inducing brain-derived neurotrophic factor and glial cell line-derived neurotrophic factor synthesis. J Neurosci Res 2004;78:250–8.
[24] Niwa M, Nitta A, Yamada Y, Nakajima A, Saito K, Seishima M, et al. An inducer for glial cell line-derived neurotrophic factor and tumor necrosis factor-alpha protects against methamphetamine-induced rewarding effects and sensitization. Biol Psychiatry 2007;61:890–901.
[25] Schiller GD, Pucilowski O, Wienicke C, Overstreet DH. Immobility-reducing effects of antidepressants in a genetic animal model of depression. Brain Res Bull 1992;28:821–3.
[26] Porsolt RD, Le Pichon M, Jalfre M. Depression: a new animal model sensitive to antidepressant treatments. Nature 1977;266:730–2.
[27] Hitoshi S, Maruta N, Higashi M, Kumar A, Kato N, Ikenaka K. Antidepressant drugs reverse the loss of adult neural stem cells following chronic stress. J Neurosci Res 2007;85:3574–85.
[28] Jones KR, Farinas I, Backus C, Reichardt LF. Targeted disruption of the BDNF gene perturbs brain and sensory neuron development but not motor neuron development. Cell 1994;76:989–99.
[29] Ibi D, Takuma K, Koike H, Mizoguchi H, Tsuritani K, Kuwahara Y, et al. Social isolation rearing-induced impairment of the hippocampal neurogenesis is associated with deficits in spatial memory and emotion-related behaviors in juvenile mice. J Neurochem 2008;105:921–32.
[30] Paxinos G, Franklin KBJ. The mouse brain in stereotaxic coordinates. San Diego: Academic Press; 2004.
[31] Manev H, Uz T, Smalheiser NR, Manev R. Antidepressants alter cell proliferation in the adult brain in vivo and in neural cultures in vitro. Eur J Pharmacol 2001;411:67–70.
[32] Chen H, Pandey GN, Dwivedi Y. Hippocampal cell proliferation regulation by repeated stress and antidepressants. Neuroreport 2006;17:863–7.
[33] Kuhn HG, Winkler J, Kempermann G, Thal LJ, Gage FH. Epidermal growth factor and fibroblast growth factor-2 have different effects on neural progenitors in the adult rat brain. J Neurosci 1997;17:5820–9.
[34] Frodl T, Schule C, Schmitt G, Born C, Baghai T, Zill P, et al. Association of the brain-derived neurotrophic factor Val66Met polymorphism with reduced hippocampal volumes in major depression. Arch Gen Psychiatry 2007;64: 410–6.
[35] Chen ZY, Jing D, Bath KG, Ieraci A, Khan T, Siao CJ, et al. Genetic variant BDNF (Val66Met) polymorphism alters anxiety-related behavior. Science 2006;314:140–3.
[36] Castren E, Voikar V, Rantamaki T. Role of neurotrophic factors in depression. Curr Opin Pharmacol 2007;7:18–21.
[37] Yang C, Xu Y, Sun N, Ren Y, Liu Z, Cao X, et al. The combined effects of the BDNF and GSK3B genes modulate the relationship between negative life events and major depressive disorder. Brain Res 2010;1355:1–6.
[38] Fortunato JJ, Reus GZ, Kirsch TR, Stringari RB, Fries GR, Kapczinski F, et al. Chronic administration of harmine elicits antidepressant-like effects and increases BDNF levels in rat hippocampus. J Neural Transm 2010;117:1131–7.
[39] Schmidt HD, Duman RS. Peripheral BDNF produces antidepressant-like effects in cellular and behavioral models. Neuropsychopharmacology 2010;35:2378–91.
[40] Eisch AJ, Bolanos CA, de Wit J, Simonak RD, Pudiak CM, Barrot M, et al. Brain-derived neurotrophic factor in the ventral midbrain-nucleus accumbens pathway: a role in depression. Biol Psychiatry 2003;54:994–1005.
[41] Marais L, Stein DJ, Daniels WM. Exercise increases BDNF levels in the striatum and decreases depressive-like behavior in chronically stressed rats. Metab Brain Dis 2009;24:587–97.
[42] Schjetnan AG, Escobar ML. In vivo BDNF modulation of hippocampal mossy fiber plasticity induced by high frequency stimulation. Hippocampus 2010 (In press).
[43] Jagasia R, Steib K, Englberger E, Herold S, Faus-Kessler T, Saxe M, et al. GABA-cAMP response element-binding protein signaling regulates maturation and survival of newly generated neurons in the adult hippocampus. J Neurosci 2009;29:7966–77.
[44] Tao X, Finkbeiner S, Arnold DB, Shaywitz AJ, Greenberg ME. Ca2+ influx regulates BDNF transcription by a CREB family transcription factor-dependent mechanism. Neuron 1998;20:709–26.
[45] Li Y, Luikart BW, Birnbaum S, Chen J, Kwon CH, Kernie SG, et al. TrkB regulates hippocampal neurogenesis and governs sensitivity to antidepressive treatment. Neuron 2008;59:399–412.
[46] Sarbassov DD, Guertin DA, Ali SM, Sabatini DM. Phosphorylation and regulation of Akt/PKB by the rictor-mTOR complex. Science 2005;307:1098–101.
[47] Nibuya M, Nestler EJ, Duman RS. Chronic antidepressant administration increases the expression of cAMP response element binding protein (CREB) in rat hippocampus. J Neurosci 1996;16:2365–72.
[48] Castro JE, Varea E, Marquez C, Cordero MI, Poirier G, Sandi C. Role of the amygdala in antidepressant effects on hippocampal cell proliferation and survival and on depression-like behavior in the rat. PLoS One 2010;5:e8618.
[49] Nasrallah HA, Hopkins T, Pixley SK. Differential effects of antipsychotic and antidepressant drugs on neurogenic regions in rats. Brain Res 2010;1354:23–9.
[50] Saarelainen T, Hendolin P, Lucas G, Koponen E, Sairanen M, MacDonald E, et al. Activation of the TrkB neurotrophin receptor is induced by antidepressant drugs and is required for antidepressant-induced behavioral effects. J Neurosci 2003;23:349–57.
[51] Gage FH. Mammalian neural stem cells. Science 2000;287:1433–8.
[52] McEwen BS. Effects of adverse experiences for brain structure and function. Biol Psychiatry 2000;48:721–31.
[53] Benraiss A, Chmielnicki E, Lerner K, Roh D, Goldman SA. Adenoviral brain-derived neurotrophic factor induces both neostriatal and olfactory neuronal recruitment from endogenous progenitor cells in the adult forebrain. J Neurosci 2001;21:6718–31.
[54] Takahashi J, Palmer TD, Gage FH. Retinoic acid and neurotrophins collaborate to regulate neurogenesis in adult-derived neural stem cell cultures. J Neurobiol 1999;38:65–81.
[55] Saruta J, Lee T, Shirasu M, Takahashi T, Sato C, Sato S, et al. Chronic stress affects the expression of brain-derived neurotrophic factor in rat salivary glands. Stress 2010;13:53–60.

[56] Naert G, Ixart G, Maurice T, Tapia-Arancibia L, Givalois L. Brain-derived neurotrophic factor and hypothalamic–pituitary–adrenal axis adaptation processes in a depressive-like state induced by chronic restraint stress. Mol Cell Neurosci 2011;46:55–66.
[57] Frey IM, Rubio-Aliaga I, Klempt M, Wolf E, Daniel H. Phenotype analysis of mice deficient in the peptide transporter PEPT2 in response to alterations in dietary protein intake. Pflugers Arch 2006;452:300–6.
[58] Treilhou M, Bras MH, Simeon N, Bayle C, Ponsot V, Couderc F. Application of CF-UV and CE-LIF to the analysis of beverages. LC–GC Eur 2001;(December):2–6.
[59] Egan MF, Kojima M, Callicott JH, Goldberg TE, Kolachana BS, Bertolino A, et al. The BDNF val66met polymorphism affects activity-dependent secretion of BDNF and human memory and hippocampal function. Cell 2003;112:257–69.
[60] Neves-Pereira M, Cheung JK, Pasdar A, Zhang F, Breen G, Yates P, et al. BDNF gene is a risk factor for schizophrenia in a Scottish population. Mol Psychiatry 2005;10:208–12.

Behavioural Brain Research 225 (2011) 222–229

Contents lists available at ScienceDirect

Behavioural Brain Research

journal homepage: www.elsevier.com/locate/bbr

Research report

Butyrylcholinesterase inhibitors ameliorate cognitive dysfunction induced by amyloid-β peptide in mice

Yoko Furukawa-Hibi[a], Tursun Alkam[a], Atsumi Nitta[a], Akihiro Matsuyama[a], Hiroyuki Mizoguchi[b], Kazuhiko Suzuki[c], Saliha Moussaoui[d], Qian-Sheng Yu[e], Nigel H. Greig[e], Taku Nagai[a], Kiyofumi Yamada[a,*]

[a] Department of Neuropsychopharmacology and Hospital Pharmacy, Nagoya University, Graduate School of Medicine, 65 Tsuruma-cho, Showa-ku, Nagoya 466-8560, Japan
[b] Futuristic Environmental Simulation Center, Research Institute of Environmental Medicine, Nagoya University, Nagoya 464-8601, Japan
[c] Translational Sciences, Novartis Pharma KK, Tokyo 106-8618, Japan
[d] Neuroscience Research, Novartis Institutes for BioMedical Research, Novartis Pharma AG, CH-4002 Basel, Switzerland
[e] Drug Design and Development Section, Laboratory of Neuroscience, Intramural Research, Program, National Institute on Aging, National Institutes of Health, Baltimore, MD 21224, USA

ARTICLE INFO

Article history:
Received 20 June 2011
Received in revised form 15 July 2011
Accepted 18 July 2011
Available online 27 July 2011

Keywords:
Acetylcholinesterase
Butyrylcholinesterase
Amyloid-β

ABSTRACT

The cholinesterase inhibitor, rivastigmine, ameliorates cognitive dysfunction and is approved for the treatment of Alzheimer's disease (AD). Rivastigmine is a dual inhibitor of acetylcholinesterase (AChE) and butyrylcholinesterase (BuChE); however, the impact of BuChE inhibition on cognitive dysfunction remains to be determined. We compared the effects of a selective BuChE inhibitor, N1-phenethyl-norcymserine (PEC), rivastigmine and donepezil (an AChE-selective inhibitor) on cognitive dysfunction induced by amyloid-β peptide ($A\beta_{1-40}$) in mice. Five-week-old imprinting control region (ICR) mice were injected intracerebroventricularly (*i.c.v.*) with either $A\beta_{1-40}$ or the control peptide $A\beta_{40-1}$ on Day 0, and their recognition memory was analyzed by a novel object recognition test. Treatment with donepezil (1.0 mg/kg), rivastigmine (0.03, 0.1, 0.3 mg/kg) or PEC (1.0, 3.0 mg/kg) 20 min prior to, or immediately after the acquisition session (Day 4) ameliorated the $A\beta_{1-40}$ induced memory impairment, indicating a beneficial effect on memory acquisition and consolidation. In contrast, none of the investigated drugs proved effective when administrated before the retention session (Day 5). Repeated daily administration of donepezil, rivastigmine or PEC, on Days 0–3 inclusively, ameliorated the cognitive dysfunction in $A\beta_{1-40}$ challenged mice. Consistent with the reversal of memory impairments, donepezil, rivastigmine or PEC treatment significantly reduced $A\beta_{1-40}$ induced tyrosine nitration of hippocampal proteins, a marker of oxidative damage. These results indicate that BuChE inhibition, as well as AChE inhibition, is a viable therapeutic strategy for cognitive dysfunction in AD.

1. Introduction

Alzheimer's disease (AD) is the leading cause of dementia in the elderly population and is characterized by progressive cognitive decline and neuropsychiatric disturbances. Accumulation of extracellular amyloid-beta (Aβ) and the formation of Aβ plaques and intracellular neurofibrillary tangles in the brain are pathological hallmarks of AD [1]. Aberrant proteolytic processing of amyloid precursor protein (APP) [2–4] results in the formation of Aβ oligomers and diffusible ligands that may damage synapses, impair memory, and ultimately induce neuronal dysfunction and neurotoxicity [5–8]. Since the major form of Aβ contains 40 amino acids ($A\beta_{1-40}$) [2–4], we and others have generated partial models of AD in rodents by intracerebroventricular (*i.c.v.*) injection of $A\beta_{1-40}$ to induce clinical signs reminiscent of AD, including learning and memory deficits and impairment of the cholinergic system [9,10].

The deficit of presynaptic markers is indication of a neuronal degeneration which is the real cause of the profound depletion of acetylcholine (ACh) within the hippocampus, basal forebrain and cortical areas [1–4]. Since changes in cholinergic regulation are a contributing factor to the cognitive dysfunction observed in AD patients, the selective acetylcholinesterase (AChE) inhibitor, donepezil, is widely utilized for symptomatic treatment of patients

Abbreviations: ACh, acetylcholine; AChE, acetylcholinesterase; APP, amyloid protein precursor; ANOVA, analysis of variance; Aβ, amyloid beta; AD, Alzheimer's disease; BuCh, butyrylcholine; BuChE, butyrylcholinesterase; ChEIs, cholinesterase inhibitors; ERK, extracellular signal-regulated kinase; *i.c.v.*, intracerebroventricular; *i.p.*, intraperitoneal; NO, nitric oxide; iNOS, inducible nitric oxide synthase; PEC, N1-phenethyl-norcymserine.

* Corresponding author. Tel.: +81 52 744 2674; fax: +81 52 744 2876.
E-mail address: kyamada@med.nagoya-u.ac.jp (K. Yamada).

0166-4328/$ – see front matter © 2011 Elsevier B.V. All rights reserved.
doi:10.1016/j.bbr.2011.07.035

[11]. The cholinesterase inhibitor rivastigmine also ameliorates cognitive dysfunction and is similarly used in the treatment of AD. Unlike donepezil, rivastigmine is a dual inhibitor of AChE and butyrylcholinesterase (BuChE) [12–14]. However, the functional relevance of BuChE inhibition in cognitive dysfunction remains largely unknown.

AChE is principally associated with neurons and axons, while BuChE is primarily expressed and secreted by glial cells within the brain [15]. Yet studies by Darvesh et al. [16,17] indicate that specific neurons use BuChE rather than AChE to cleave presynaptic ACh. Indeed, some 10–15% of cholinergic neurons in the human hippocampus and amygdala express BuChE in their cell bodies and proximal dendrites, in lieu of AChE [16,17]. In the healthy human brain, AChE and BuChE are found in the ratio of 4:1. However, in the brains of AD patients AChE activity can decline by up to 45% during disease progression, reflecting the disappearance of neurons and axons to which it is associated, while BuChE activity can be elevated by up to 2-fold [17], thereby altering this ratio considerably.

Highly selective, reversible, central nervous system (CNS)-penetrable BuChE inhibitors, e.g., N1-phenethyl-norcymserine (PEC) and its analogues, have recently been developed and are permitting elucidation of the physiological role of brain BuChE. Selective BuChE inhibition has been shown to elevate cortical extracellular ACh levels in rats in a manner similar to that achieved by selective AChE inhibition using donepezil or by dual AChE/BuChE inhibition using rivastigmine [18]. In addition to elevating brain ACh, PEC has been shown to augment long-term potentiation (LTP; a molecular correlate of learning), improve cognitive performance in aged healthy rats, and lower brain levels of $A\beta_{1-40}$ and $A\beta_{1-42}$ in transgenic mice overexpressing human Aβ [19]. However, the effect of selective BuChE inhibition on Aβ-induced cognitive dysfunction remains unclear.

Aβ is widely recognized to mediate oxidative stress in the brain, particularly in AD [20,21]. An increase in protein nitration, a marker of widespread oxidative damage, is correlated with the severity of cognitive dysfunction in humans as well as animals [22–27]. We have previously demonstrated that continuous *i.c.v.* infusion of $A\beta_{1-40}$ stimulates a time-dependent expression of inducible nitric oxide synthase (iNOS) and an overproduction of nitric oxide (NO) within the rat hippocampus [28]. In addition, tyrosine nitration contributes to Aβ-induced, and oxidative damage-mediated, cognitive dysfunction in rats and mice [29–32]. Recently, we have also demonstrated that tyrosine nitration of hippocampal proteins, specifically neurofilament light chain, correlates with the severity of cognitive impairments in mice [29,31].

In the present study we compared the effects of rivastigmine and PEC with those of donepezil on cognitive dysfunction in Aβ-injected mice using a novel object recognition test, and investigated any correlation with oxidative damage via tyrosine nitration of hippocampal proteins.

2. Materials and methods

2.1. Animals

Male, 5-week-old imprinting control region (ICR) mice were used throughout the study (Nihon SLC Co., Shizuoka, Japan). They were housed in a controlled environment (23 ± 1 °C, 50 ± 5% humidity), maintained on a 9:00 a.m. to 9:00 p.m. light cycle and allowed access to food and water *ad libitum*. All experiments were performed in accordance with the *Guidelines for Animal Experiments* of Nagoya University Graduate School of Medicine. All animal procedures and care conformed to the *Guidelines for Proper Conduct of Animal Experiments* (Science Council of Japan, 2006).

2.2. Treatment and experimental design

$A\beta_{1-40}$ (obtained from Bachem, Bubendorf, Switzerland) was dissolved in saline to a stock concentration of 1.0 mg/ml and stored at −20 °C before use. The reverse peptide, $A\beta_{40-1}$ (Bachem) was utilized as a control and prepared in the same way. The dissolved stock solutions of $A\beta_{1-40}$ and $A\beta_{40-1}$ peptides were incubated at 37 °C for 4 days, to allow aggregation prior to administration [31]. Incubated $A\beta_{1-40}$, or $A\beta_{40-1}$ was administered by *i.c.v.* injection as described previously [29,31,33,34]. Briefly, a microsyringe with a 28-gauge stainless-steel needle 3.0 mm long was used for all experiments. Mice were anesthetized lightly with ether, and the needle was inserted unilaterally 1 mm to the right of the midline point, at an equal distance between the eyes and the ears and perpendicular to the plane of the skull. Thereafter, an *i.c.v.* injection of 5 μl peptide (5 μg) or vehicle was delivered gradually over 3 min. Mice recovered rapidly and within 1 min post-injection exhibited normal behavior. The administration site was confirmed in preliminary experiments and neither the insertion of the needle, nor the volume of injection, significantly influenced survival, behavioral response or cognitive function.

Donepezil (Aricept™; Eisai, Tokyo, Japan) and rivastigmine (Exelon®, Novartis Pharma AG, Basel, Switzerland) were dissolved in saline. PEC (kindly supplied by Dr. Nigel H. Greig, synthesized to >99.9% chiral and chemical purity [35] to provide a characterized compound with an IC_{50} value for BuChE: 5 nM and AChE: <30 μM) was dissolved in saline containing 0.05% ethanol and 0.15% Tween 80. Donepezil (0.3, 1.0 mg/kg), rivastigmine (0.03, 0.3, 1.0 mg/kg) and PEC (1.0, 3.0 mg/kg) were administered via the intraperitoneal (*i.p.*) route at various time points before and during the different phases of the novel object recognition test (described in Section 2.4).

2.3. Locomotor activity

Locomotor activity was measured using an infrared detector (Neuroscience Company, Tokyo, Japan) in a plastic box (32 × 22 × 15 cm), as described previously [36]. Mice were injected with donepezil (0.3, 1.0 mg/kg), rivastigmine (0.03, 0.3, 1.0 mg/kg) or PEC (1.0, 3.0 mg/kg) and the locomotor activity was measured for 60 min.

2.4. Novel object recognition test

Novel object recognition analysis was performed on Days 3–5 after the *i.c.v.* injection of $A\beta_{1-40}$ (Day 0) [29,37]. This method has been previously used as a measure of cognitive dysfunction in mouse models of natural aging and AD [38]. A plastic chamber (35 × 35 × 35 cm) was used in low light conditions during the light phase of the light/dark cycle. The procedure consisted of three different phases: a habituation phase, an acquisition phase and a retention phase. On Day 3 (habituation phase), mice were individually subjected to a single familiarization session of 10 min, during which time they were introduced into the empty arena to become familiar with the apparatus. On Day 4 (acquisition phase), the animals were subjected to a single 10 min session, during which two floor-fixed objects (A and B) were placed in a symmetric position from the center of the arena, 15 cm apart from one another and 8 cm from the nearest wall. Mice were allowed to explore the objects in the open field. On Day 5 (retention phase), mice were allowed to explore the open field in the presence of two objects: the familiar object A and a novel object C, each of a different shape and color but of similar size (A and C). A recognition index, calculated for each mouse, was expressed as the ratio (TC × 100)/(TA+TC), where TA and TC are the times spent during the retention phase on object A and object C.

The time spent exploring individual object (nose pointing toward the object at a distance ≤1 cm) was recorded by a blinded investigator. Drug and vehicle treatments were administrated once *i.p.*, either 20 min before the acquisition phase, immediately after the acquisition phase, or 20 min before the retention phase. Alternatively, the drugs were administered once a day for 4 days (Day 0–3 inclusively) after *i.c.v.* injection of $A\beta_{1-40}$ and then the mice were subjected to novel object recognition analysis on Days 3–5 as before.

2.5. Sample preparation for Western blot analysis

Removed hippocampus were placed on an ice-cold glass plate and immediately frozen and stored at −80 °C. Hippocampal protein extracts were obtained by homogenization in ice-cold radioimmunoprecipitation assay (RIPA) lysis buffer containing 20 mM Tris–HCl (pH 7.6), 150 mM sodium chloride, 2 mM EDTA–2Na, 50 mM sodium fluoride, 1 mM sodium vanadate, 1% (v/v) Nonidet P-40, 1% (w/v) sodium deoxycholate, 0.1% (w/v) sodium dodecyl sulfate (SDS). The RIPA buffer was supplemented with complete protease inhibitor cocktail tablets (Roche Applied Science, Mannheim, Germany). Homogenates were centrifuged at 13,000 × *g* for 20 min to obtain the desired supernatant of the extracts.

2.6. Western blot analysis

Following protein content analysis by Lowry method, equal amounts (20 μg) of protein sample were resolved by 10% SDS–polyacrylamide gel electrophoresis and transferred to a polyvinylidene difluoride membrane (Millipore, MA, USA) for 1 h with 15 V. Membranes were incubated in 3% (w/v) skimmed milk in phosphate-buffered saline containing 0.05% (v/v) Tween 20 for 2 h at room temperature, and probed with anti-nitrotyrosine mouse monoclonal 1A6 antibody (1:1000 diluted in 3% (w/v) skimmed milk, Millipore, catalog number 05-233) for overnight at 4 °C and anti-β-actin goat polyclonal antibody (1:1000 diluted in 3% (w/v) skimmed milk) for 1 h at room temperature (Santa Cruz Biotechnology Inc., Santa Cruz, CA,

USA). Immunoreactive complexes on the membrane were detected using Enhanced Chemiluminescence Plus Western Blotting Detection Reagents (GE Healthcare Japan, Tokyo, Japan) and analyzed by Atto Light-Capture system (Atto, Tokyo, Japan). Exposure time was 3 min.

2.7. Statistical analysis

All results are expressed as mean ± standard error (SE) values. Statistical significance was determined with a one-way analysis of variance (ANOVA) followed by the Bonferroni's multiple comparisons test, with $p < 0.05$ as the threshold to define a significant level of difference.

3. Results

3.1. Effects of donepezil, rivastigmine and PEC on baseline locomotor activity

Donepezil (0.3, 1.0 mg/kg), PEC (1.0, 3.0 mg/kg) and rivastigmine (0.03 mg/kg) had no significant effect on baseline locomotor activity. At higher doses (0.3 and 1.0 mg/kg) rivastigmine significantly decreased locomotor activity in a dose-dependent manner ($p < 0.05$, $p < 0.001$ *vs.* control mice, respectively, Fig. 1).

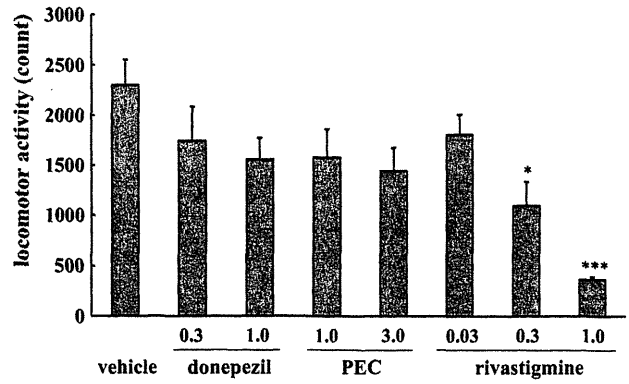

Fig. 1. Effects of donepezil, rivastigmine and PEC on baseline locomotor activity in mice. Mice were injected *i.p.* with donepezil (0.3, 1.0 mg/kg), rivastigmine (0.03, 0.1, 0.3 mg/kg) or PEC (1.0, 3.0 mg/kg) and the baseline locomotor activity was measured over 60 min, in the absence of Aβ peptide injection. Control mice were injected (*i.p.*) with saline. Values indicate the mean ± SE ($n = 5$). $F(7,32) = 5.736$, $p < 0.001$; $^{*}p < 0.05$ and $^{***}p < 0.001$ vs. control.

3.2. Effects of a single administration of donepezil, rivastigmine and PEC on cognitive dysfunction induced by $A\beta_{1-40}$ in mice

Mice were challenged with $A\beta_{1-40}$ by *i.c.v.* injection and their cognitive ability was examined using a novel object recognition paradigm. First, the effect of cholinesterase inhibitors (ChEIs) on memory acquisition was investigated. Donepezil (1.0 mg/kg), rivastigmine (0.03, 0.1, 0.3 mg/kg) or PEC (1.0, 3.0 mg/kg) was administered *i.p.* 20 min before the acquisition phase on Day 4 (Fig. 2A). The time exploring the two objects during the acquisition session (Day 4) was unaffected by $A\beta_{1-40}$, $A\beta_{40-1}$, donepezil or PEC treatment (Table 1). Rivastigmine (0.03 and 0.1 mg/kg) similarly had no effect, but the drug at a dose of 0.3 mg/kg significantly reduced interaction time with the two objects compared with saline-treated $A\beta_{1-40}$ controls ($p < 0.001$, Table 1). During the retention phase of the task (Day 5), mice challenged with $A\beta_{1-40}$ proved unable to discriminate between the unfamiliar and familiar objects, and displayed a significantly decreased recognition index compared with those challenged with the control reverse peptide, $A\beta_{40-1}$ ($p < 0.001$, Fig. 2B and C). Treatment with donepezil, rivastigmine or PEC 20 min before acquisition fully ameliorated the $A\beta_{1-40}$-induced impairment of memory recognition ($p < 0.001$ for all drugs at all doses vs. saline-treated $A\beta_{1-40}$ controls, Fig. 2B and C).

The effect of ChEIs on memory consolidation was then investigated. When donepezil, rivastigmine or PEC was administered immediately after the acquisition session on Day 4 (Fig. 3A), they significantly ameliorated the $A\beta_{1-40}$ induced cognitive dysfunction compared with the saline-injected $A\beta_{1-40}$ control mice ($p < 0.001$ for all drugs at all doses vs. saline-treated $A\beta_{1-40}$ controls, except for rivastigmine 0.3 mg/kg where $p < 0.05$, Fig. 3B and C).

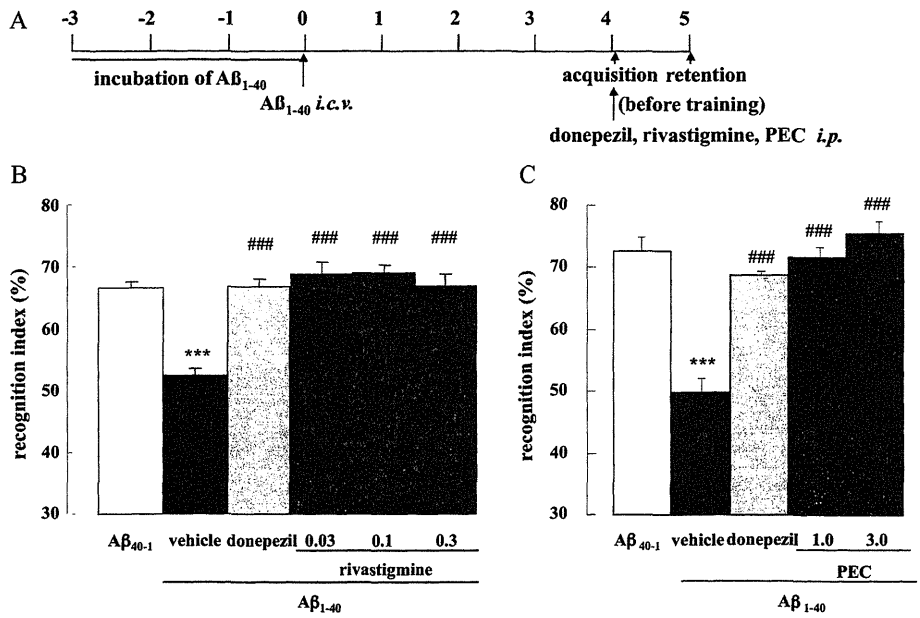

Fig. 2. Effects of donepezil, rivastigmine and PEC on memory acquisition in $A\beta_{1-40}$-injected mice. Mice were injected with $A\beta_{1-40}$ on Day 0, and subjected to the novel object recognition task on Days 4–5 (A). Donepezil (1.0 mg/kg), rivastigmine (0.03, 0.1, 0.3 mg/kg) or PEC (1.0, 3.0 mg/kg) were administered *i.p.* 20 min before the acquisition session on Day 4 (B and C). Values indicate the mean ± SE ($n = 8$ for B, $n = 8$ for C). $F(5,42) = 18.4$, $p < 0.001$ (B); $F(4,35) = 28.32$, $p < 0.001$ (C); $^{***}p < 0.001$ vs. $A\beta_{40-1}$ control; $^{###}p < 0.001$ vs. vehicle-treated $A\beta_{1-40}$ control.

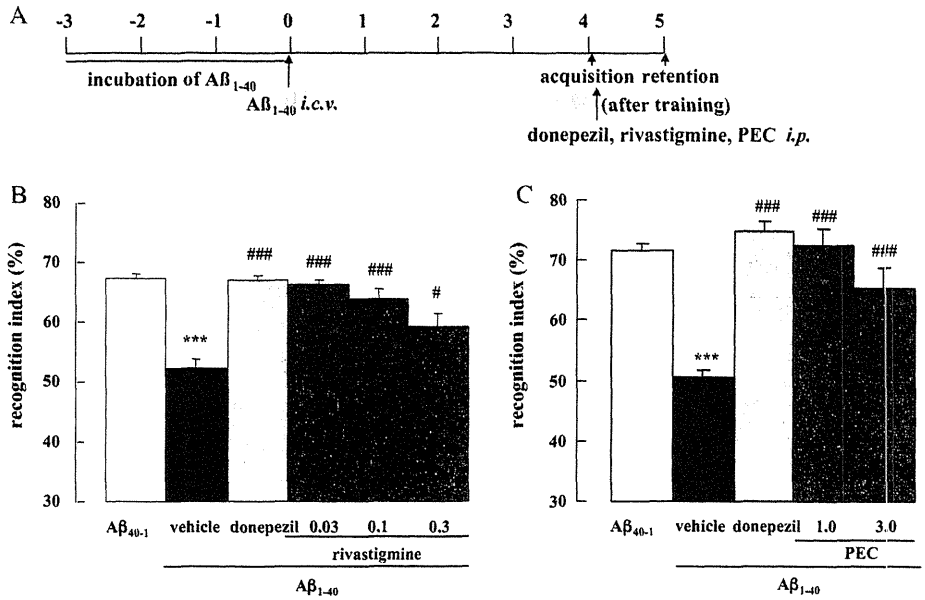

Fig. 3. Effect of donepezil, rivastigmine and PEC on memory consolidation in $A\beta_{1-40}$-injected mice. Mice were injected with $A\beta_{1-40}$ on Day 0 and subjected to the novel object recognition task on Day 4–5 (A). Donepezil (1.0 mg/kg), rivastigmine (0.03, 0.1, 0.3 mg/kg) or PEC (1.0, 3.0 mg/kg) were administered *i.p.* immediately after the acquisition session on Day 4 (B and C). Values indicate the mean ± SE ($n = 8$ for B, $n = 6$ for C). $F(5,42) = 17.99$, $p < 0.001$ (B); $F(4,26) = 25.25$, $p < 0.001$ (C); $^{***}p < 0.001$ vs. $A\beta_{40-1}$ control; $^{\#}p < 0.05$ and $^{\#\#\#}p < 0.001$ vs. vehicle-treated $A\beta_{1-40}$ control.

Finally the effect of ChEIs on memory retrieval was investigated. When donepezil, rivastigmine or PEC was administered 20 min before the retention session on Day 5 (Fig. 4A), none of the drugs improved the cognitive dysfunction induced by $A\beta_{1-40}$ (Fig. 4B and C), in contrast to the previous dosing regimens

3.3. Amelioration of an $A\beta_{1-40}$-induced cognitive dysfunction by repeated daily administration of donepezil, rivastigmine or PEC

Subsequently, we evaluated the effects of repeated daily treatment of donepezil (1.0 mg/kg), rivastigmine (0.03 mg/kg) or PEC (1.0 mg/kg) on memory impairment induced by $A\beta_{1-40}$. No intergroup differences were evident with regard to the overall object exploration time during the acquisition session (data not shown). During the retention phase (Day 5), mice challenged with $A\beta_{1-40}$ and administered saline proved unable to discriminate between unfamiliar and familiar objects, and displayed a significantly decreased recognition index in comparison with the reverse-peptide controls ($p < 0.001$ and $p < 0.01$ for treatment groups A and B, respectively, Fig. 5A–C). Repeated treatment with donepezil, rivastigmine and PEC significantly enhanced new object discrimination in $A\beta_{1-40}$-injected mice ($p < 0.001$ for all drugs vs. saline-treated $A\beta_{1-40}$ controls, Fig. 5B and C), fully ameliorating the impairment.

Table 1
Effects of donepezil, rivastigmine and PEC on the combined exploration time of two objects during the acquisition session in the novel object recognition test.

	Drug	Dose (mg/kg)	Time (s)
Treatment group A			
$A\beta_{40-1}$	Saline	–	39.6 ± 1.4
$A\beta_{1-40}$	Saline	–	42.2 ± 1.4
$A\beta_{1-40}$	Donepezil	1.0	42.0 ± 1.3
$A\beta_{1-40}$	Rivastigmine	0.03	41.0 ± 0.9
$A\beta_{1-40}$	Rivastigmine	0.1	39.2 ± 1.4
$A\beta_{1-40}$	Rivastigmine	0.3	19.0 ± 2.7***
Treatment group B			
$A\beta_{40-1}$	Saline	–	56.0 ± 4.1
$A\beta_{1-40}$	Saline	–	57.0 ± 6.1
$A\beta_{1-40}$	Donepezil	1.0	50.3 ± 4.2
$A\beta_{1-40}$	PEC	1.0	55.5 ± 3.8
$A\beta_{1-40}$	PEC	3.0	65.9 ± 3.6

Mice were injected with $A\beta_{1-40}$ on Day 0, and were subjected to the novel object recognition test on Day 3–5. Donepezil (1.0 mg/kg), rivastigmine (0.03, 0.1, 0.3 mg/kg) and saline (A) or donepezil (1.0 mg/kg), PEC (1.0, 3.0 mg/kg) or saline (B) were administered *i.p.* 20 min before the acquisition session on Day 4. Values indicate the mean ± SE ($n = 8$ for A, $n = 5$ for B). $F(5,42) = 31.67$, $p < 0.001$ (A); $F(4,20) = 1.98$, $p = 0.137$ (B); $^{***}p < 0.001$ vs. saline-treated $A\beta_{1-40}$.

3.4. Tyrosine nitration of proteins induced by $A\beta_{1-40}$ in the hippocampus of mice

We have previously demonstrated that memory impairment induced by $A\beta_{1-40}$ in mice is associated with an increase in oxidative stress and tyrosine nitration of hippocampal proteins [31]. Accordingly, we evaluated the effects of repeated daily treatments of donepezil, rivastigmine and PEC on tyrosine nitration of hippocampal proteins. Injection of $A\beta_{1-40}$ *i.c.v.* induced extensive tyrosine nitration compared with $A\beta_{40-1}$, which was detected as a single band of approximately 70 kDa ($p < 0.05$ vs. $A\beta_{40-1}$ control, Fig. 6). Repeated 4-day treatments with donepezil, rivastigmine and PEC fully reduced the elevated tyrosine nitration generated by $A\beta_{1-40}$ ($p < 0.05$ for all drugs vs. saline-treated $A\beta_{1-40}$ controls, Fig. 6). By contrast, acute treatment with donepezil, rivastigmine or PEC failed to change the levels of tyrosine nitration of hippocampal proteins (data not shown).

4. Discussion

In the current study, the independent roles of BuChE and AChE in the cholinergic amelioration of Alzheimer-associated cognitive impairment were evaluated, using a novel object recognition paradigm. This behavioral test is considered to involve visual learning and recognition processing, which are particularly affected during AD [39,40]. Aggregated $A\beta_{1-40}$ oligomers have been previously shown to impair LTP and synapse formation and induce neuronal dysfunction using *in vitro* and *in vivo* model systems [5–8]. Following *i.c.v.* injection of aggregated $A\beta_{1-40}$ into the brains of

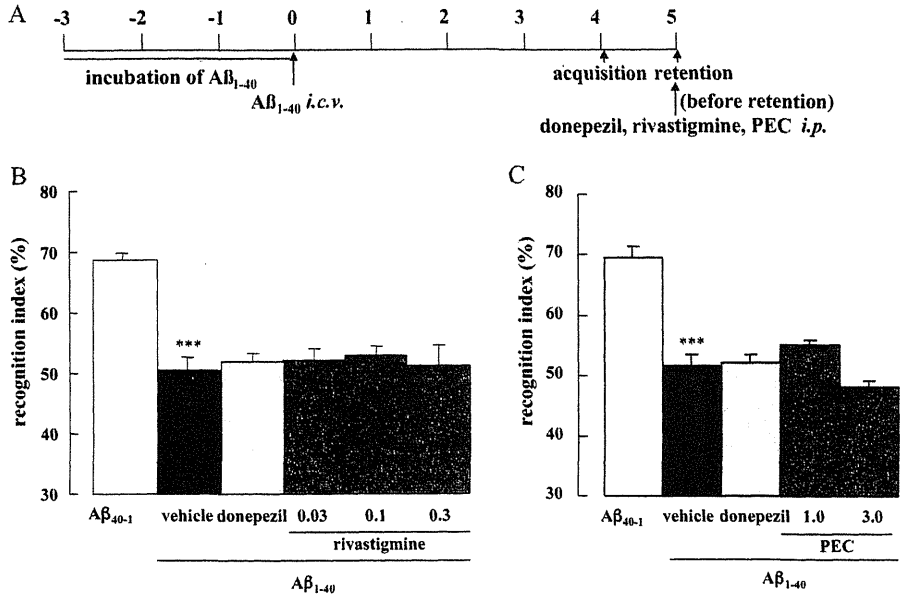

Fig. 4. Effect of donepezil, rivastigmine and PEC on memory retrieval in $A\beta_{1-40}$-injected mice. Mice were injected with $A\beta_{1-40}$ on Day 0 and subjected to the novel object recognition task on Day 4–5 (A). Donepezil (1.0 mg/kg), rivastigmine (0.03, 0.1, 0.3 mg/kg) or PEC (1.0, 3.0 mg/kg) were administered *i.p.* 20 min before the retention session on Day 5 (B and C). Values indicate the mean ± SE ($n = 6$ for B, $n = 4$ for C). $F(5,30) = 11.76$, $p < 0.001$ (B); $F(4,11) = 24.56$, $p < 0.001$ (C); $^{***}p < 0.001$ vs. $A\beta_{40-1}$ control.

mice in our model of AD, a clear and consistent deficit in recognition index was apparent when measured 4 days later, in accordance with prior studies [9,10,41]. We demonstrate for the first time that a selective BuChE inhibitor, PEC, completely reversed the cognitive impairment induced by $A\beta_{1-40}$, in a way comparable to that achieved by either selective AChE inhibition (donepezil) or by dual inhibition of AChE and BuChE (rivastigmine). A single treatment with donepezil, rivastigmine or PEC reversed the impairment of recognition memory when mice were treated 20 min before, or immediately after, the acquisition session. However, when these same drugs were administrated 20 min before the retention phase, they had no impact on memory impairment in $A\beta_{1-40}$-challenged mice. Wise et al. [42] examined the effect of donepezil on spatial memory by radial-arm maze task and demonstrated that donepezil (0.3 and 1.0 mg/kg) improved spatial memory when administered 20 min before the acquisition session. Alternatively, when given immediately after the acquisition phase or 30 min prior to the retention test, donepezil failed to affect spatial memory [43]. These results together with our present findings suggest that both AChE and BuChE inhibitors, separately (i.e., donepezil and PEC) or in

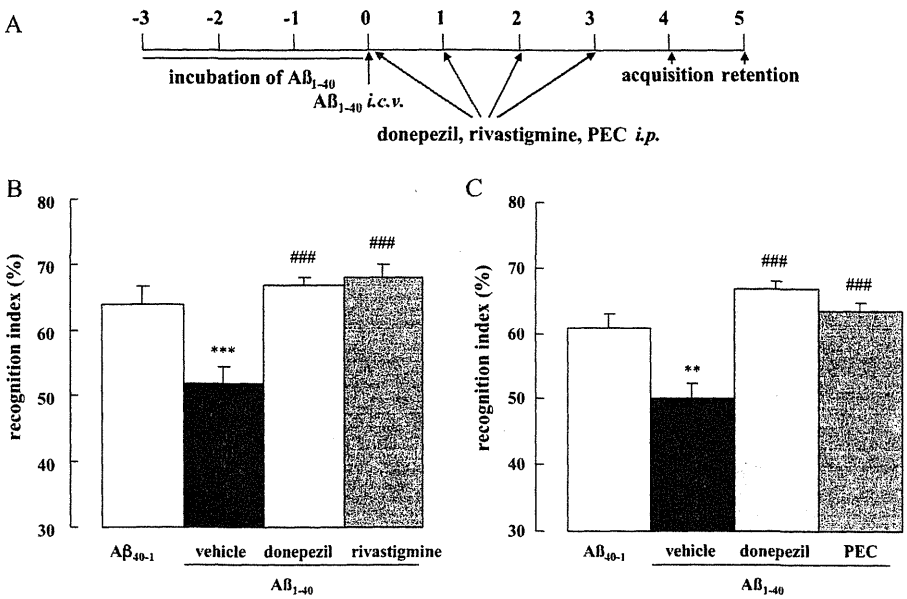

Fig. 5. Effect of repeated treatment with donepezil, rivastigmine and PEC on cognitive dysfunction in $A\beta_{1-40}$-injected mice. Donepezil (1.0 mg/kg), rivastigmine (0.3 mg/kg) and PEC (1.0 mg/kg) were repeatedly administered *i.p.* once a day for 4 days, starting immediately after the *i.c.v.* injection of $A\beta_{1-40}$ on Day 0. The mice were subjected to the novel object recognition task on Day 4–5. Values indicate the mean ± S.E. ($n = 8$ for B, $n = 10$ for C). $F(3,29) = 42.28$, $p < 0.001$ (B); $F(3,40) = 9.42$, $p < 0.001$ (C); $^{**}p < 0.01$ and $^{***}p < 0.001$ vs. $A\beta_{40-1}$ control; $^{###}p < 0.001$ vs. vehicle-treated $A\beta_{1-40}$ control.

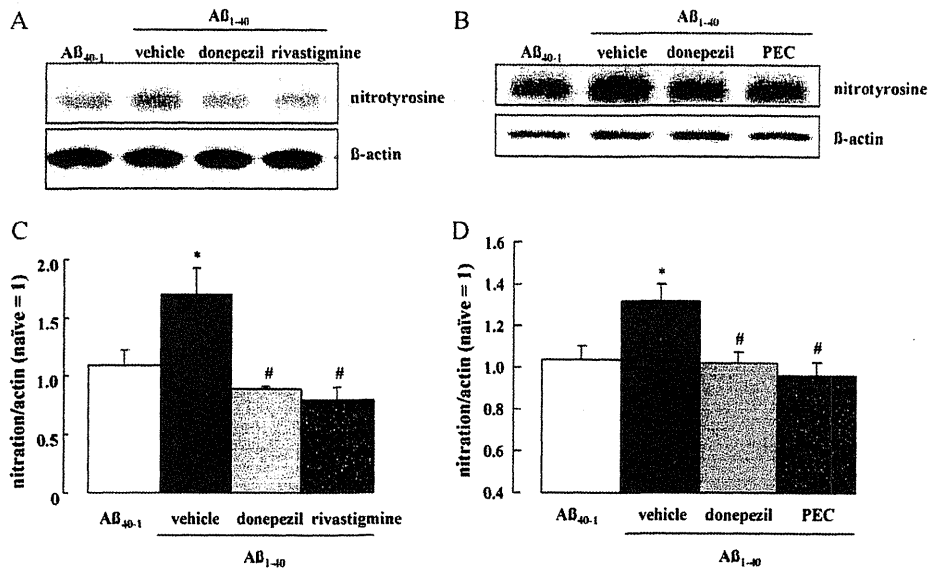

Fig. 6. Effect of repeated treatment with donepezil, rivastigmine and PEC on tyrosine nitration of hippocampal protein in $A\beta_{1-40}$-injected mice. Donepezil (1.0 mg/kg), rivastigmine (0.3 mg/kg) and PEC (1.0 mg/kg) were repeatedly administered once a day for 4 days, starting immediately following the *i.c.v.* injection of $A\beta_{1-40}$ on Day 0. On Day 4, tyrosine nitration of hippocampal proteins was analyzed by Western blotting. Values indicate the mean ± SE ($n = 8$ for C, $n = 15$ for D). $F(3,28) = 4.77$, $p < 0.01$ (C); $F(3,56) = 3.968$, $p < 0.05$ (D); $^{*}p < 0.05$ vs. $A\beta_{40-1}$ control; $^{\#}p < 0.05$ vs. vehicle-treated $A\beta_{1-40}$ control.

combination (i.e., rivastigmine), have beneficial effects on memory impairment induced by $A\beta_{1-40}$, likely through an action on memory acquisition and/or consolidation, but not via the process of memory retrieval. Moreover, it has been reported that PEC at the dose of 5 mg/kg induced an increase in cortical extracellular ACh levels with a moderate BuChE inhibition [18]. Greig et al. [19] have also demonstrated that the extracellular ACh level in rat parietal cortex slightly but significantly increase after PEC (1.25 mg/kg) treatment. Since the doses of PEC (1.0, 3.0 mg/kg) used in this experiment have been previously shown to have no effect on AChE activity [18,19], ameliorative effect of PEC on Aβ-induced cognitive impairment may be associated with transient increase in extracellular level of ACh through BChE inhibition. Interestingly, it has been noted by Wise et al. [42] that the combination of two effective drugs with separate mechanisms at subthreshold doses can provide synergistic action. Since rivastigmine inhibits both of AChE and BuChE, the effective dose of rivastigmine (0.03 mg/kg) that ameliorated memory impairment in our study proved lower than that of donepezil (1.0 mg/kg) and PEC (1.0 mg/kg). It remain unclear if the effective dose of rivastigmine increase ACh level in the brain although approximately 2–3 fold increases in cortical extracellular ACh level has been detected followed the administration of the drug at the dose of 0.6 mg/kg [18]. Furthermore, whether or not such a benefit of dual cholinesterase inhibitor vs. a selective one would translate into any clinically relevant difference remains unknown. These points should be addressed in future studies.

Similarly, repeated daily treatment with donepezil, rivastigmine or PEC for 4 days, fully reversed the memory impairment induced by $A\beta_{1-40}$. The mechanism(s) underpinning this action remain to be elucidated but are likely different from that associated with the cognitive improvement evident after acute treatment. The repeated drug treatments ended 24 h before the acquisition phase, at a time when the cholinergic actions of all the assessed drugs are predicted to be minimal. In contrast, the single acute administration of the same drugs closer to the time of the acquisition phase, produced elevated brain ACh levels during acquisition [18]. A potential mechanism underlying the behavioral improvements provided by repeated administration of AChE and BuChE inhibitors may derive from protection against the $A\beta_{1-40}$ challenge that induces behavioral deficit.

During the early stages of AD pathology, peroxynitrite-mediated damage is associated with progressive cognitive impairment [22,43–45]. It has been reported that injection of preaggregated $A\beta_{1-42}$ peptide into the nucleus basalis magnocellularis of rats results in an increase in the level of iNOS immunoreactivity through cyclooxygenase-2 induction [46]. Recent proteomic studies have identified several protein targets of oxidative modification in rat brain injected with $A\beta_{1-42}$ into the nucleus basalis magnocellularis [47]. Aβ upregulates iNOS, mediating peroxynitrite protein damage via hyperphosphorylation of extracellular signal-regulated kinase (ERK), while the selective inhibition of ERK or iNOS abolishes Aβ-induced neurotoxicity [48,49] and memory impairment [50].

More specifically, our previous studies indicate an involvement of tyrosine nitration of hippocampal proteins, especially neurofilament light chain, by Aβ peptides [29–31], which was associated with memory impairment in Aβ-challenged mice [31]. We subsequently investigated whether treatment with ChEIs could alter this observed nitration of hippocampal proteins. Repeated daily treatment with donepezil, rivastigmine and PEC prevented the increase in tyrosine nitration of proteins in the hippocampus while ameliorating $A\beta_{1-40}$-induced memory impairment. In contrast, single administration of the same agents failed to affect the tyrosine nitration of hippocampal proteins in similarly challenged mice, implicating the involvement of cholinergically-mediated neuroprotective actions with repeated administration. ACh has known anti-inflammatory actions; therefore it is possible that increased expression of AChE and BuChE reduces ACh levels, triggering a process of inflammation, characteristic of AD [51,52]. The restoration of such balance by AChE and/or BuChE inhibition may have the potential to mitigate pro-inflammatory signaling cascades. Hwang et al. [53] suggested that donepezil may attenuate microglial production of NO and tumor necrosis factor-α (TNF-α) and suppress iNOS, interleukin-1-β, and TNF-α gene expression. Together with results in the current study, these findings suggest that inflammatory responses, including tyrosine nitration of proteins, may be reduced by chronic therapeutic treatment with AChE and/or BuChE inhibitors.

5. Conclusions

In the current study, we demonstrated that both selective BuChE inhibition mediated by PEC, and selective AChE inhibition mediated by donepezil, provide beneficial effects on the cognitive dysfunction apparent in $A\beta_{1-40}$-challenged mice. Furthermore, the dual AChE/BuChE inhibitor rivastigmine also demonstrated beneficial effects on memory acquisition and consolidation. This may involve direct classical cholinergic augmentation, together with a cholinergically-mediated protective action, potentially via the reduction of inflammation.

These data support further investigation of dual AChE/BuChE inhibition in preclinical and clinical studies to maximize therapeutic efficacy, and the evaluation of selective BuChE inhibition as a new therapeutic strategy for cognitive dysfunction in AD.

Acknowledgements

This study was supported in part by the following funding sources: (i) grants-in-aid for Scientific Research (No. 22390046, 23659135) from the Japan Society for the Promotion of Science; (ii) a grant from the global COE program from the Ministry of Education, Culture, Sports, Science and Technology of Japan; (iii) a grant from the Academic Frontier Project for Private Universities, matching fund subsidy from MEXT, 2007–2011; (iv) a grant from the Regional Joint Research Program supported by grants to Private Universities to Cover Current Expenses from the Ministry of Education, Culture, Sports, Science and Technology (MEXT); (v) a grant from Novartis Pharma KK and ONO Pharmaceutical Co., Ltd. (vi) The Intramural Research Program of the National Institute on Aging, National Institutes of Health.

References

[1] Small DH, McLean CA. Alzheimer's disease and the amyloid beta protein: what is the role of amyloid? J Neurochem 1999;73:443–9.
[2] Estus S, Golde TE, Kunishita T, Blades D, Lowery D, Eisen M, et al. Potentially amyloidogenic, carboxyl-terminal derivatives of the amyloid protein precursor. Science 1992;255:726–8.
[3] Golde TE, Estus S, Younkin LH, Selkoe DJ, Younkin SG. Processing of the amyloid protein precursor to potentially amyloidogenic derivatives. Science 1992;255:728–30.
[4] Haass C, Schlossmacher MG, Hung AY, Vigo-Pelfrey C, Mellon A, Ostaszewski BL, et al. Amyloid beta-peptide is produced by cultured cells during normal metabolism. Nature 1992;359:322–5.
[5] Yankner BA, Dawes LR, Fisher S, Villa-Komaroff L, Oster-Granite ML, Neve RL. Neurotoxicity of a fragment of the amyloid precursor associated with Alzheimer's disease. Science 1989;245:417–20.
[6] Pike CJ, Walencewicz AJ, Glabe CG, Cotman CW. Aggregation-related toxicity of synthetic beta-amyloid protein in hippocampal cultures. Eur J Pharmacol 1991;207:367–8.
[7] Pike CJ, Walencewicz AJ, Glabe CG, Cotman CW. In vitro aging of beta-amyloid protein causes peptide aggregation and neurotoxicity. Brain Res 1991;563:311–4.
[8] Howlett DR, Jennings KH, Lee DC, Clark MS, Brown F, Wetzel R, et al. Aggregation state and neurotoxic properties of Alzheimer beta-amyloid peptide. Neurodegeneration 1995;4:23–32.
[9] McDonald MP, Dahl EE, Overmier JB, Mantyh P, Cleary J. Effects of an exogenous beta-amyloid peptide on retention for spatial learning. Behav Neural Biol 1994;62:60–7.
[10] Yamada K, Nitta A, Saito T, Hu J, Nabeshima T. Changes in ciliary neurotrophic factor content in the rat brain after continuous intracerebroventricular infusion of beta-amyloid(1–40) protein. Neurosci Lett 1995;201:155–8.
[11] Small DH, Mok SS, Bornstein JC. Alzheimer's disease and Abeta toxicity: from top to bottom. Nat Rev Neurosci 2001;2:595–8.
[12] Bullock R, Lane R. Executive dyscontrol in dementia, with emphasis on subcortical pathology and the role of butyrylcholinesterase. Curr Alzheimer Res 2007;4:277–93.
[13] Naik RS, Hartmann J, Kiewert C, Duysen EG, Lockridge O, Klein J. Effects of rivastigmine and donepezil on brain acetylcholine levels in acetylcholinesterase-deficient mice. J Pharm Pharm Sci 2009;12:79–85.
[14] Touchon J, Bergman H, Bullock R, Rapatz G, Nagel J, Lane R. Response to rivastigmine or donepezil in Alzheimer's patients with symptoms suggestive of concomitant Lewy body pathology. Curr Med Res Opin 2006;22:49–59.
[15] Mesulam M, Guillozet A, Shaw P, Quinn B. Widely spread butyrylcholinesterase can hydrolyze acetylcholine in the normal and Alzheimer brain. Neurobiol Dis 2002;9:88–93.
[16] Darvesh S, Grantham DL, Hopkins DA. Distribution of butyrylcholinesterase in the human amygdala and hippocampal formation. J Comp Neurol 1998;393:374–90.
[17] Darvesh S, Hopkins DA, Geula C. Neurobiology of butyrylcholinesterase. Nat Rev Neurosci 2003;4:131–8.
[18] Cerbai F, Giovannini MG, Melani C, Enz A, Pepeu G. N1phenethyl-norcymserine a selective butyrylcholinesterase inhibitor, increases acetylcholine release in rat cerebral cortex: a comparison with donepezil and rivastigmine. Eur J Pharmacol 2007;572:142–50.
[19] Greig NH, Utsuki T, Ingram DK, Wang Y, Pepeu G, Scali C, et al. Selective butyrylcholinesterase inhibition elevates brain acetylcholine, augments learning and lowers Alzheimer beta-amyloid peptide in rodent. Proc Natl Acad Sci USA 2005;102:17213–8.
[20] Butterfield DA, Drake J, Pocernich C, Castegna A. Evidence of oxidative damage in Alzheimer's disease brain: central role for amyloid beta-peptide. Trends Mol Med 2001;7:548–54.
[21] Sultana R, Butterfield DA. Role of oxidative stress in the progression of Alzheimer's disease. J Alzheimers Dis 2010;19:341–53.
[22] Smith MA, Richey Harris PL, Sayre LM, Beckman JS, Perry G. Widespread peroxynitrite-mediated damage in Alzheimer's disease. J Neurosci 1997;17:2653–7.
[23] Lim GP, Chu T, Yang F, Beech W, Frautschy SA, Cole GM. The curry spice curcumin reduces oxidative damage and amyloid pathology in an Alzheimer transgenic mouse. J Neurosci 2001;21:8370–7.
[24] Perry G, Nunomura A, Hirai K, Zhu X, Perez M, Avila J, et al. Is oxidative damage the fundamental pathogenic mechanism of Alzheimer's and other neurodegenerative diseases? Free Radic Biol Med 2002;33:1475–9.
[25] Kim HC, Yamada K, Nitta A, Olariu A, Tran MH, Mizuno M, et al. Immunocytochemical evidence that amyloid beta (1-42) impairs endogenous antioxidant systems in vivo. Neuroscience 2003;119:399–419.
[26] Andersen JK. Oxidative stress in neurodegeneration: cause or consequence? Nat Med 2004;10(Suppl):S18–25.
[27] Walsh DM, Selkoe DJ. Deciphering the molecular basis of memory failure in Alzheimer's disease. Neuron 2004;44:181–93.
[28] Tran MH, Yamada K, Olariu A, Mizuno M, Ren XH, Nabeshima T. Amyloid beta-peptide induces nitric oxide production in rat hippocampus: association with cholinergic dysfunction and amelioration by inducible nitric oxide synthase inhibitors. FASEB J 2001;15:1407–9.
[29] Alkam T, Nitta A, Mizoguchi H, Itoh A, Nabeshima T. A natural scavenger of peroxynitrites, rosmarinic acid, protects against impairment of memory induced by Abeta(25–35). Behav Brain Res 2007;180:139–45.
[30] Alkam T, Nitta A, Mizoguchi H, Saito K, Seshima M, Itoh A, et al. Restraining tumor necrosis factor-alpha by thalidomide prevents the amyloid beta-induced impairment of recognition memory in mice. Behav Brain Res 2008;189:100–6.
[31] Alkam T, Nitta A, Mizoguchi H, Itoh A, Murai R, Nagai T, et al. The extensive nitration of neurofilament light chain in the hippocampus is associated with the cognitive impairment induced by amyloid beta in mice. J Pharmacol Exp Ther 2008;327:137–47.
[32] Tran MH, Yamada K, Nakajima A, Mizuno M, He J, Kamei H, et al. Tyrosine nitration of a synaptic protein synaptophysin contributes to amyloid beta-peptide-induced cholinergic dysfunction. Mol Psychiatry 2003;8:407–12.
[33] Maurice T, Lockhart BP, Privat A. Amnesia induced in mice by centrally administered beta-amyloid peptides involves cholinergic dysfunction. Brain Res 1996;706:181–93.
[34] Alkam T, Nitta A, Furukawa-Hibi Y, Niwa M, Mizoguchi H, Yamada K, et al. Oral supplementation with Leu-Ile, a hydrophobic dipeptide, prevents the impairment of memory induced by amyloid beta in mice via restraining the hyperphosphorylation of extracellular signal-regulated kinase. Behav Brain Res 2010;210:184–90.
[35] Yu Q, Holloway HW, Utsuki T, Brossi A, Greig NH. Synthesis of novel phenserine-based-selective inhibitors of butyrylcholinesterase for Alzheimer's disease. J Med Chem 1999;42:1855–61.
[36] Nakajima A, Yamada K, Nagai T, Uchiyama T, Miyamoto Y, Mamiya T, et al. Role of tumor necrosis factor-alpha in methamphetamine-induced drug dependence and neurotoxicity. J Neurosci 2004;24:2212–25.
[37] Nagai T, Takuma K, Kamei H, Ito Y, Nakamichi N, Ibi D, et al. Dopamine D1 receptors regulate protein synthesis-dependent long-term recognition memory via extracellular signal-regulated kinase 1/2 in the prefrontal cortex. Learn Mem 2007;14:117–25.
[38] Nitta A, Itoh A, Hasegawa T, Nabeshima T. Beta-Amyloid protein-induced Alzheimer's disease animal model. Neurosci Lett 1994;170:63–6.
[39] Haley GE, Berteau-Pavy F, Berteau-Pavy D, Raber J. Novel image-novel location object recognition task sensitive to age-related cognitive decline in nondemented elderly. Age (Dordr) 2011.
[40] Werheid K, Clare L. Are faces special in Alzheimer's disease? Cognitive conceptualisation, neural correlates, and diagnostic relevance of impaired memory for faces and names. Cortex 2007;43:898–906.
[41] Games D, Khan KM, Soriano FG, Keim PS, Davis DL, Bryant K, et al. Lack of Alzheimer pathology after beta-amyloid protein injections in rat brain. Neurobiol Aging 1992;13:569–76.
[42] Wise LE, Iredale PA, Stokes RJ, Lichtman AH. Combination of rimonabant and donepezil prolongs spatial memory duration. Neuropsychopharmacology 2007;32:1805–12.

[43] Luth HJ, Munch G, Arendt T. Aberrant expression of NOS isoforms in Alzheimer's disease is structurally related to nitrotyrosine formation. Brain Res 2002;953:135–43.
[44] Vodovotz Y, Lucia MS, Flanders KC, Chesler L, Xie QW, Smith TW, et al. Inducible nitric oxide synthase in tangle-bearing neurons of patients with Alzheimer's disease. J Exp Med 1996;184:1425–33.
[45] Webster B, Hansen L, Adame A, Crews L, Torrance M, Thal L, et al. Astroglial activation of extracellular-regulated kinase in early stages of Alzheimer disease. J Neuropathol Exp Neurol 2006;65:142–51.
[46] Giovannini MG, Scali C, Prosperi C, Bellucci A, Vannucchi MG, Rosi S, et al. Beta-amyloid-induced inflammation and cholinergic hypofunction in the rat brain in vivo: involvement of the p38MAPK pathway. Neurobiol Dis 2002;11: 257–74.
[47] Boyd-Kimball D, Castegna A, Sultana R, Poon HF, Petroze R, Lynn BC, et al. Proteomic identification of proteins oxidized by Abeta(1-42) in synaptosomes: implications for Alzheimer's disease. Brain Res 2005;1044: 206–15.
[48] Nathan C, Calingasan N, Nezezon J, Ding A, Lucia MS, La Perle K, et al. Protection from Alzheimer's-like disease in the mouse by genetic ablation of inducible nitric oxide synthase. J Exp Med 2005;202:1163–9.
[49] Rapoport M, Ferreira A. PD98059 prevents neurite degeneration induced by fibrillar beta-amyloid in mature hippocampal neurons. J Neurochem 2000;74:125–33.
[50] Diaz A, Mendieta L, Zenteno E, Guevara J, Limon ID. The role of NOS in the impairment of spatial memory and damaged neurons in rats injected with amyloid beta 25–35 into the temporal cortex. Pharmacol Biochem Behav 2011;98:67–75.
[51] Rao AA, Sridhar GR, Das UN. Elevated butyrylcholinesterase and acetylcholinesterase may predict the development of type 2 diabetes mellitus and Alzheimer's disease. Med Hypotheses 2007;69:1272–6.
[52] Rosas-Ballina M, Tracey KJ. Cholinergic control of inflammation. J Intern Med 2009;265:663–79.
[53] Hwang J, Hwang H, Lee HW, Suk K. Microglia signaling as a target of donepezil. Neuropharmacology 2010;58:1122–9.

Experimental Eye Research 93 (2011) 873–879

Contents lists available at SciVerse ScienceDirect

Experimental Eye Research

journal homepage: www.elsevier.com/locate/yexer

Periocular injection of *in situ* hydrogels containing Leu–Ile, an inducer for neurotrophic factors, promotes retinal ganglion cell survival after optic nerve injury

Masayoshi Nakatani [a,*], Yuko Shinohara [a], Miki Takii [a], Hisato Mori [a], Nobuharu Asai [a], Shigeru Nishimura [a], Yoko Furukawa-Hibi [b], Yoshiaki Miyamoto [c], Atsumi Nitta [c]

[a] *Bioengineering Institute, Research & Development Division, Nidek Co., Ltd., 13-2 Hama-cho, Gamagori, Aichi 443-0036, Japan*
[b] *Department of Neuropsychopharmacology & Hospital Pharmacy, Nagoya University Graduate School of Medicine, Nagoya 466-8850, Japan*
[c] *Department of Pharmaceutical Therapy & Neuropharmacology, Faculty of Pharmaceutical Science, Graduate School of Medicine and Pharmaceutical Science, University of Toyama, Toyama 930-0194, Japan*

ARTICLE INFO

Article history:
Received 26 April 2011
Accepted in revised form
30 September 2011
Available online 8 October 2011

Keywords:
Leu–Ile
periocular injection
neurotrophic factor
optic nerve injury
retinal ganglion cell

ABSTRACT

Intraocular administration of neurotrophic factors has been shown to delay irreversible degeneration of retinal ganglion cells (RGCs). It would be beneficial for the treatment of optic nerve (ON) injury if such neurotrophic factors could be delivered in a less-invasive manner. The dipeptide leucine–isoleucine (Leu–Ile) appears to induce the production of neurotrophic factors, including brain-derived neurotrophic factor (BDNF) and glial cell line-derived neurotrophic factor (GDNF), in the brain. We therefore administered Leu–Ile via periocular depot injection in rats and investigated the dipeptide's ability to induce BDNF and GDNF in the retina and to delay RGC loss in an ON injury model. Poloxamer–alginate hydrogels containing Leu–Ile were injected into the subconjunctival space of intact or ON-injured rats. BDNF and GDNF levels in the retina were determined by an enzyme immunoassay. Survival of RGCs was assessed in retinal flatmounts. Activation of extracellular signal-regulated kinases (ERK) and cAMP response element binding protein (CREB) in the retina was examined by Western blotting. At 2 h after injection of fluorescein isothiocyanate-conjugated Leu–Ile, the fluorescence intensities in the retina were 4.3-fold higher than those in the saline control. Treatment with Leu–Ile significantly increased the retinal levels of BDNF at 6 h and GDNF at 6–72 h after injection. Treatment with Leu–Ile significantly increased RGC survival to 14 days after ON injury and enhanced the activation of ERK at 72 h and CREB at 48 h after injection in the ON-injured retina. These results suggest that periocular delivery of Leu–Ile induces BDNF and GDNF production in the retina, which may eventually enhance RGC survival after ON injury.

1. Introduction

Damage to the optic nerve (ON) results in retrograde degeneration of retinal ganglion cells (RGCs), which may lead to visual loss. Unfortunately, there is no established treatment modality to preserve the RGCs and axons in optic neuropathies such as glaucoma. One of the mechanisms proposed to explain this RGC loss is a reduction in the levels of neurotrophic factors that those neurons receive from the brain via retrograde axonal transport (Dahlmann-Noor et al., 2010; Weber et al., 2010). Among these factors, exogenous brain-derived growth factor (BDNF) and glial cell line-derived neurotrophic factor (GDNF) have been shown to delay RGC loss after axotomy and ON crush in cats and rodents (Koeberle and Ball, 1998; Parrilla-Reverter et al., 2009; Dahlmann-Noor et al., 2010). Moreover, combined treatment with BDNF and GDNF promotes better survival of RGCs than does either factor used individually (Yan et al., 1999; Koeberle and Ball, 2002). However, the task of adequately delivering these macromolecules to the retina is challenging due to limited access to the retina and blood–ocular barriers. Systemic administration might deliver these factors to the retina, but this also carries a higher risk of untoward side effects. Intravitreal administration is an effective means of delivering therapeutic levels of these factors quickly with minimal systemic side effects, but it is an invasive procedure with complications such as cataract formation, vitreous hemorrhage, and endophthalmitis. Moreover, any RGC survival promoting effect after direct injection of neurotrophic factors into the eye is transient. Although periocular injection is a clinically well-tolerated and less-invasive

* Corresponding author. Tel.: +81 533 66 3030; fax: +81 533 66 3185.
E-mail address: masayoshi_nakatani@nidek.co.jp (M. Nakatani).

0014-4835/$ – see front matter © 2011 Elsevier Ltd. All rights reserved.
doi:10.1016/j.exer.2011.09.024

method than the intravitreal approach, it would be difficult for macromolecules to reach the retina and exhibit their survival promoting effects if administered in this manner.

We have reported that leucine–isoleucine (Leu–Ile), a hydrophobic dipeptide, induces BDNF and GDNF synthesis both in the striatum and in cultured mesencephalic neurons (Nitta et al., 2004). Leu–Ile also protects the brain from damage caused by administration of 6-hydroxydopamine and methamphetamine (Nitta et al., 2004; Niwa et al., 2007). In addition, Leu–Ile is known to increase GDNF expression through the Akt/cAMP response element binding protein (CREB), which is activated by the heat shock protein 90/Akt signaling pathway (Cen et al., 2006). Leu–Ile may thus be an effective small molecule for treating optic neuropathies. It is necessary, however, to ensure safe and adequate delivery to the target tissues to enable this dipeptide to be used as a therapeutic agent.

Poloxamer 407, a copolymer of ethylene oxide and propylene oxide blocks, exhibits *in situ* gelling behavior owing to its thermoreversible properties. The formulation has led to prolonged release profiles for many drug applications (Dumortier et al., 2006) as well as to the reduction of peptide degradation in tissues (Wenzel et al., 2002). In ocular applications, Poloxamer 407 is well-tolerated in periocular injection (Vehanen et al., 2007).

In the present study, we attempted to induce BDNF and GDNF in the retina by periocular injection of Leu–Ile by using a poloxamer-based solution as the vehicle, and investigated their effects on degeneration of RGCs after ON crush injury in rats.

2. Materials and methods

2.1. Preparation of in situ hydrogel containing Leu–Ile

Poloxamer 407 and sodium alginate were obtained from Sigma–Aldrich Japan (Tokyo, Japan). Poloxamer was added to cold 0.2% sodium alginate under continuous stirring until a homogenous solution was obtained (Vehanen et al., 2007; Lin et al., 2004). The final concentration of poloxamer was 20%. The polymer solution was autoclaved at 121 °C for 15 min. Leu–Ile or fluorescein isothiocyanate (FITC) conjugated Leu–Ile (FITC–Leu–Ile), prepared by American Peptide Company, Inc. (Sunnyvale, CA, USA), was dissolved in the poloxamer–alginate solution. The solutions were adjusted to a pH in the range of 6.8–7.4 with NaOH.

2.2. Animals

Wistar rats (Japan SLC, Shizuoka, Japan) were used in accordance with the ARVO Statement for the Use of Animals in Ophthalmic and Vision Research in protocols approved and monitored by the Institutional Animal Care and Use Committee of Nidek Co., Ltd. The animals were housed in a 12-h light and 12-h dark cycle and given standard chow and water *ad libitum*.

2.3. Periocular injections in rats

Male Wistar rats (8 weeks old, 240–275 g body weight) were anesthetized with a combination of ketamine (80 mg/kg) and xylazine (7 mg/kg) by intraperitoneal injection. One of the following solutions was injected into the temporal subconjunctival space using a 25-gauge needle with a glass syringe: 40 μL of the poloxamer–alginate solution, 0.9% saline containing FITC–Leu–Ile (0.17 μmol), or the poloxamer solution containing 0.8, 8.0, or 80 mM Leu–Ile (0.03, 0.33, and 3.3 μmol, respectively). The concentrations of Leu–Ile were chosen based on a preliminary study in which intravitreal injection of 0.03 μmol Leu–Ile remarkably increased both BDNF and GDNF levels in the retina (15.7-fold and 6.3-fold increase compared with saline vehicle injection, respectively). Each eye received one injection. The solution was kept on an ice block before injection to ensure that it was in liquid form. The animals were euthanized at the indicated times after injection by cutting the abdominal aorta under diethyl ether anesthesia, and the eyes were enucleated.

2.4. Fluorescence measurements

The sclera, choroid/retinal pigment epithelium (RPE), and retina were isolated from the eyeball. The ONs (between the optic chiasm and the eyeball) were removed from the brain. Each tissue was homogenized on ice with 500 μL PBS (pH 7.4) using a homogenizer (HG30; Hitachi Koki, Tokyo, Japan) for the sclera and ON, and an ultrasonicator (Sonifier250; Branson Japan, Tokyo, Japan) for the choroid/RPE and retina. The homogenate was allowed to sit on ice for 2 h, and then centrifuged at 14,000 *g* for 5 min. Fluorescence intensities (excitation at 495 nm, emission at 525 nm) of the supernatants were determined directly using a microplate spectrofluorometer (SpectraMax M2e; Molecular Devices Japan, Tokyo, Japan). Measurements were calibrated by measuring the fluorescence of serial dilutions of FITC–Leu–Ile standards, with corrections made for tissue autofluorescence using the values for an untreated eye.

2.5. Enzyme immunoassay

Levels of BDNF and GDNF protein expression were determined by enzyme immunoassay (EIA) (Nitta et al., 2004). Homogenate buffer (0.1 M Tris–HCl, pH 7.4) containing 1 M NaCl, 2% bovine serum albumin, 2 mM EDTA, and 0.2% sodium nitride was added to the retinal tissue at a ratio of 1 g wet tissue to 19 mL of buffer, pulse-sonicated for 100 s, and centrifuged at 100,000 *g* for 30 min. The supernatant was collected and used for the EIA.

2.6. Optic nerve crush injury and periocular injection

The rats were anesthetized with intraperitoneal injection of sodium pentobarbital (45 mg/kg). An incision was made in the temporal conjunctiva of the right eye, and the lateral rectus muscle was detached under an operating microscope. The optic nerve was exposed and isolated. Care was taken to avoid damaging small vessels around the optic nerve. A vascular clip (40 g micro-vascular clip; Bear Medic, Ibaraki, Japan) was then applied to the optic nerve at a distance of 1–2 mm posterior to the globe for 10 s to cause a crush injury (Karim et al., 2009). To confirm that retinal vessels retained patency, the retina was examined under an operating microscope immediately after the insult. The dissected conjunctiva was pushed back in place, and the eyelid sutured at the temporal canthus. At 30 min after the ON crush, 40 μL of the poloxamer–alginate solution containing 8 or 80 mM Leu–Ile was injected into the nasal subconjunctival space. The nasal side was selected to minimize leakage of the formed gel depot from the incision site.

2.7. Quantification of retinal ganglion cell rescue

The survival of RGCs was quantified by FluoroGold (FG; Biotium, Hayward, CA, USA) retrograde labeling of retinal flatmounts. After the rats were anesthetized with a mixture of ketamine and xylazine, 4 μL of FG dissolved in distilled water to a concentration of 2% was injected into the superior colliculus bilaterally at the following coordinates: 6.0 mm posterior to the bregma, 1.5 mm lateral to the midline, and 4.0 mm under the skull. This FG-labeling was conducted 3 days before euthanizing the rats in order to avoid overcounting RGCs by mistaking dye-engulfing macrophages and

microglia for labeled RGCs (Maeda et al., 2004; Tsai et al., 2008). The eyes were harvested from euthanized animals and fixed with 4% paraformaldehyde for 2 h. The isolated whole retinas were flat-mounted vitreous side up on a microscope slide, and examined under a 400× epifluorescence microscope (E800; Nikon, Tokyo, Japan) equipped with a filter set (excitation filter: 350–400 nm, barrier filter: 515 nm). FG-labeled RGCs were counted on a fluorescent digital micrograph in a masked fashion. On the micrograph, the retina was divided into twelve standard areas, with three areas (0.336 mm^2 in total) in each quadrant at 1, 2, and 3 mm from the optic nerve head. The density of labeled RGCs (cells/mm^2) was calculated for each retina from the average of 12 counts.

2.8. Western blotting

Western blot analysis of phosphorylated ERK and CREB was performed with modifications as described by Alkam et al. (2010). Briefly, the retinal tissues were homogenized in ice-cold extraction buffer (20 mM Trizma hydrochloride buffer [pH 7.6] containing 150 mM sodium chloride, 2 mM EDTA-2Na, 50 mM sodium fluoride, 10 mM sodium vanadate, 1% Nonidet P-40, 1% sodium deoxycholate, 0.1% sodium dodecyl sulfate [SDS], 1 mg/mL pepstatin, 1 mg/mL aprotinin, and 1 mg/mL leupeptin). Equal amounts of protein, 20 μg/lane, were resolved by 10% SDS–polyacrylamide gel electrophoresis, and then transferred to a polyvinylidene difluoride membrane (Millipore, Billerica, MA, USA). Membranes were incubated in 3% bovine serum albumin in phosphate-buffered saline containing 0.05% (v/v) Tween 20 for 2 h at room temperature. They were then independently incubated at 4 °C overnight with anti-ERK(1/2) phospho-threonine202/tyrosine204(pERK) rabbit antibody (Cell Signaling Technology, Beverley, MA, USA), anti-ERK(1/2) rabbit antibody (Cell Signaling Technology), anti-phospho-CREB rabbit antibody (Cell Signaling Technology), or anti-CREB rabbit antibody (Cell Signaling Technology). Next, the labeled proteins were allowed to react with horseradish peroxidase-conjugated anti-rabbit IgG (Amersham Biosciences, Piscataway, NJ, USA), and then readied for visualization by chemiluminescence (Western blotting detection reagents, Amersham Biosciences) according to the manufacturer's instructions. Quantification was performed using the image analysis software ImageQuant TL (GE Healthcare UK Ltd, Amersham, England).

2.9. Statistical analysis

All data are expressed as mean ± SEM. Statistical differences between two groups were determined with Student's *t* test. Statistical differences among three or more groups were determined with Dunnett's multiple comparison test. $P < 0.05$ was regarded as statistically significant.

3. Results

3.1. Leu–Ile amounts in tissue extractions

To estimate permeability of Leu–Ile into the posterior segments, poloxamer–alginate or saline containing FITC–Leu–Ile (0.17 μmol) was injected subconjunctivally in rat eyes. The poloxamer–alginate solution immediately formed a gel at the injection site. Table 1 shows the amount of FITC–Leu–Ile in extracts of sclera, choroid/RPE, retina, and optic nerve. In both the saline and poloxamer–alginate groups, the values were highest in the sclera and gradiently decreased toward the choroid/RPE, retina, and optic nerve at 2 h after injection. Compared with the saline group, the values of the poloxamer–alginate group were 14.4-fold, 15.0-fold, 4.3-fold, and 15.8-fold higher in the sclera, choroid/RPE, retina, and optic nerve, respectively.

Table 1
Amount of FITC–Leu–Ile in the posterior tissues of the eye after periocular injection in rats.

Time after injection	Tissue	FITC–Leu–Ile (pmol/tissue)	
		Saline	Poloxamer–alginate
2 h	Sclera	110.56 ± 17.70	1591.55 ± 120.29*
	Choroid/RPE	10.55 ± 1.98	158.27 ± 37.66*
	Retina	9.67 ± 2.65	41.53 ± 3.39*
	Optic nerve	0.70 ± 0.24	11.05 ± 3.89*
6 h	Sclera	10.16 ± 1.46	8.85 ± 1.06
	Choroid/RPE	0.62 ± 0.18	0.76 ± 0.19
	Retina	0.72 ± 0.11	0.91 ± 0.13
	Optic nerve	0.58 ± 0.09	1.20 ± 0.30

Data represented as mean ± SEM ($n = 4$–6 per group). FITC–Leu–Ile was injected into the subconjunctival space of intact rats. FITC–Leu–Ile, fluorescein isothiocyanate-conjugated Leu–Ile; RPE, retinal pigment epithelium. *: $P < 0.01$ vs. saline group.

However, they had decreased to levels comparable with those of the saline control by 6 h after injection.

3.2. Effect of Leu–Ile to induce production of BDNF and GDNF in retina

The time-course of BDNF and GDNF levels in the retina was examined by performing EIA at 6, 24, and 72 h after periocular injection of 3.3 μmol Leu–Ile into rat eyes. BDNF levels at 6 h were higher than those in the vehicle (hydrogel)-treated rats (Fig. 1A). GDNF levels increased 6–72 h after Leu–Ile treatment (Fig. 1B). Dose-response at 6 h revealed that 0.03 and 0.33 μmol Leu–Ile injection increased GDNF levels, while 3.3 μmol Leu–Ile injection increased both BDNF and GDNF levels compared with vehicle-only injection. Vehicle injection, however, also increased BDNF and GDNF levels compared with the saline control (Fig. 1C and D).

3.3. Effects of Leu–Ile to promote RGC survival in ON crush injury

RGC density in intact rat eyes was 2327 ± 36/mm^2 (cells/mm^2; mean ± SEM). By 14 days after ON crush, with saline or vehicle injection, RGC densities had decreased to 1105 ± 110/mm^2 and 1213 ± 88/mm^2, respectively. The eyes treated with 0.33 μmol Leu–Ile showed a greater RGC density (1752 ± 62/mm^2) compared with that of the saline/vehicle-treated group. Treatment with 3.3 μmol Leu–Ile also resulted in a higher RGC density (1563 ± 114/mm^2) compared with the saline/vehicle treatment (Fig. 2).

3.4. Effects of Leu–Ile on activation of ERK and CREB in ON-injured retina

To explore Leu–Ile-induced signal transduction in ON-injured retinas, activation of ERK and CREB were determined by Western blotting (Figs. 3 and 4). The activation of ERK and CREB was not altered in intact retinas or in ON-injured retinas with saline-treatment. Slight enhancement of ERK activation was observed in ON-injured retinas at 48 and 72 h after vehicle treatment (compared with normal). Treatment with 3.3 μmol Leu–Ile resulted in greater enhancement of ERK activation in ON-injured retinas at 48 h (compared with normal) and 72 h (compared with normal/saline/vehicle). Leu–Ile treatment also enhanced CREB activation in ON-injured retinas at 48 h (compared with normal/saline/vehicle).

4. Discussion

To estimate the penetration of Leu–Ile into the eye, we investigated changes in fluorescence in different posterior segments after periocular injection of poloxamer–alginate hydrogels containing

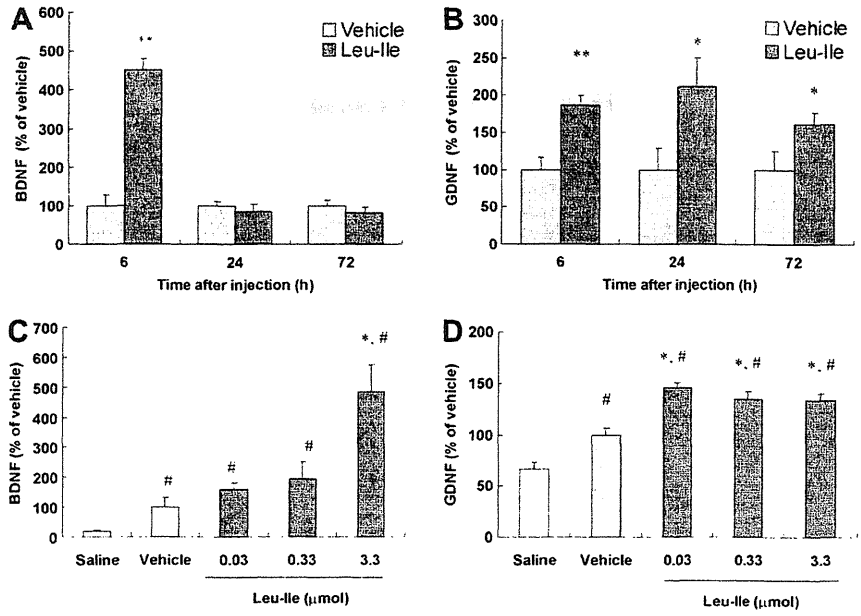

Fig. 1. Changes in BDNF (A, C) and GDNF (B, D) levels in rat retina after periocular injection of Leu–Ile. (A, B) Time-course of effects for 3.3 μmol Leu–Ile. Compared with the vehicle (hydrogel) group, both BDNF and GDNF levels were elevated at 6 h after treatment, but only GDNF levels remained elevated until 72 h. Data represented as mean ± SEM ($n = 7$–8 per group). **: $P < 0.01$, *: $P < 0.05$ vs. vehicle group. (C, D) Dose-response of Leu–Ile effects 6 h after treatment. BDNF levels were elevated with 3.3 μmol Leu–Ile, whereas GDNF levels were elevated with 0.03, 0.33, and 3.3 μmol Leu–Ile compared with the saline/vehicle group. Data represented as mean ± SEM ($n = 6$ per group). *: $P < 0.01$ vs. vehicle group; #: $P < 0.01$ vs. saline group.

FITC–Leu–Ile. We observed that the hydrogels remained on the sclera and enhanced Leu–Ile's permeability into the retina, which was the target tissue in this study, at 2 h after injection. By 6 h after injection, however, the hydrogels had become invisible on the sclera, and fluorescence in the tissues returned to levels comparable to those of the saline control (Table 1). Vehanen et al. (2007) have reported that periocular injection of 20% poloxamer solution facilitates absorption of small molecules (376 Da) into rat eye more

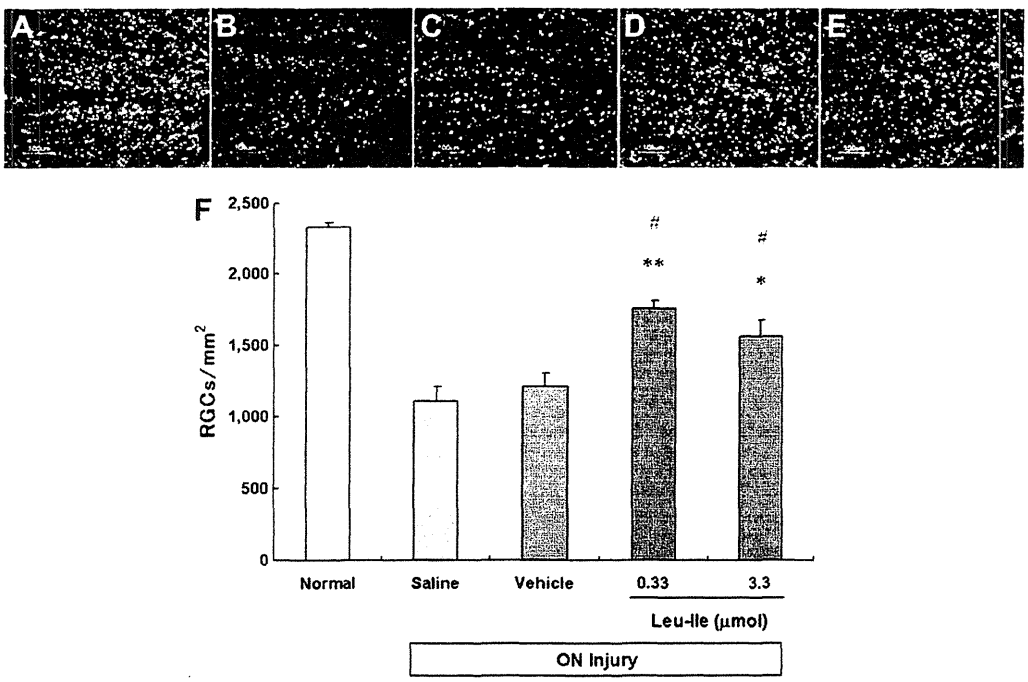

Fig. 2. Micrographs of flat-mounted retinas with retrograde labeling by FluoroGold and a graph showing RGC-rescue effects of periocular injection of Leu–Ile after optic nerve (ON) injury in rats. (A–E) Representative flat-mounted preparations of central areas of retinas. (A) Normal; (B) saline-treated with ON injury; (C) vehicle-treated with ON injury; (D) 0.33 μmol Leu–Ile-treated with ON injury; (E) 3.3 μmol Leu–Ile-treated with ON injury; (F) Density (in cells per square millimeter) of FluoroGold-labeled RGCs at 14 days after ON injury. Retinas treated with 0.33 and 3.3 μmol Leu–Ile showed higher RGC densities compared with saline/vehicle groups. Data represented as mean ± SEM ($n = 9$–10 per group). **: $P < 0.01$, *: $P < 0.05$ vs. vehicle group; #: $P < 0.01$ vs. saline group.

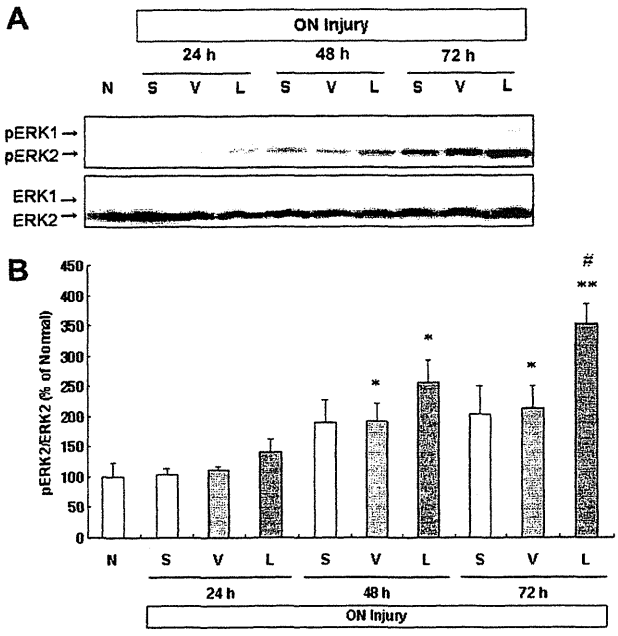

Fig. 3. Western blot analysis of pERK in rat retinas with optic nerve (ON) injury after periocular injection of Leu–Ile. (A) ERK phosphorylation was elevated in ON-injured retinas at 72 h after 3.3 μmol Leu–Ile treatment compared with saline/vehicle groups. N, Normal; S, Saline; V, Vehicle; L, Leu–Ile. (B) Densitometric analysis of ERK. The phosphorylation status of ERK2 is shown as the ratio of phosphorylated proteins to unphosphorylated proteins. Data represented as mean ± SEM ($n = 4$ per group). **: $P < 0.01$, *: $P < 0.05$ vs. normal; #: $P < 0.05$ vs. saline/vehicle groups.

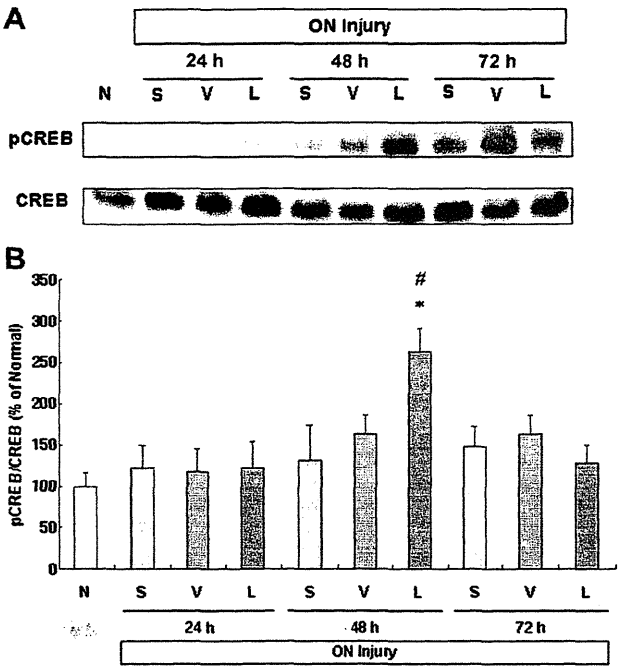

Fig. 4. Western blot analysis of pCREB in rat retinas with optic nerve (ON) injury after periocular injection of Leu–Ile. (A) CREB phosphorylation was elevated in ON-injured retinas at 48 h after 3.3 μmol Leu–Ile treatment compared with saline/vehicle groups. (B) Densitometric analysis of CREB. The phosphorylation status of CREB is shown as the ratio of phosphorylated proteins to unphosphorylated proteins. Data represented as mean ± SEM ($n = 4$ per group). *: $P < 0.01$ vs. normal; #: $P < 0.05$ vs. saline/vehicle groups.

effectively than larger molecules (4–40 kDa). However, the molecules' release from the poloxamer and absorption into the vitreous body only lasted for approximately 3 h. This relatively short-term interaction was also seen in our study. We used FITC–Leu–Ile because native Leu–Ile is a living component and is difficult to quantify in tissues. One possible limitation in our study is that our results may not precisely reflect the permeability of Leu–Ile into the eye because the molecular size of FITC–Leu–Ile is three times that of native Leu–Ile (244 Da). We confirmed in an *in vitro* experiment, however, that 80% of Leu–Ile is released into PBS from hydrogels containing 40 mM Leu–Ile within 8 h (data not shown). Our *in vivo* data are qualitatively similar to the quick-release profile found *in vitro*. Rieke et al. (2010) have reported that good correlation was obtained between their *in vitro* and *in vivo* release experiments when fluorescently-labeled protein was injected subconjunctivally using thermosetting hydrogel. We may therefore conjecture that the use of poloxamer–alginate as the vehicle improves bioavailability of Leu–Ile in a relatively short period of time. What would be more desirable, however, is more prolonged and controlled delivery.

Treatment with 3.3 μmol Leu–Ile increased BDNF and GDNF levels in the retina as early as at 6 h (Fig. 1). These results suggest that Leu–Ile can rapidly penetrate the blood–retinal barrier and reach target tissues at bioactive levels with this approach. Increased GDNF levels lasted for at least 3 days after the treatment, but increased levels of BDNF were not sustained. In addition, only GDNF levels increased with 0.03 μmol Leu–Ile, which was the lowest dose tested. The response was not dose-dependent. Cen et al. (2006) have reported that Leu–Ile binds to heat shock cognate protein 70 (Hsc70) and modulation of Hsc70 by this dipeptide triggers the transmission of neurotrophic signals, resulting in upregulation of GDNF expression. In rat retina, Hsc70 is strongly expressed in all layers, except the outer segments (Dean et al., 1999). Similarly, binding of Leu–Ile to Hsc70 seems to affect the increase of GDNF in retina. GDNF induction by Leu–Ile likely involves combinatorial interactions with multiple transcription factors. Moreover, Leu–Ile can also bind with other not yet defined proteins (unpublished data). Therefore, the lack of dose–response relationship may be attributed to the complicated cellular mechanisms underlying the GDNF-inducing effect of Leu–Ile. To investigate the effects of Leu–Ile on RGC survival, we tested two doses of Leu–Ile: 0.33 μmol, which stimulated only GDNF, and 3.3 μmol, which stimulated both BDNF and GDNF in intact rats. Treatment with Leu–Ile enhanced RGC survival, although there was no significant difference between the two dose groups (Fig. 2). These results may imply that the GDNF stimulated by Leu–Ile is principally involved in RGC-rescue.

Western blotting revealed that Leu–Ile had activated the ERK and CREB signaling pathways in ON-injured retinas by 48 and/or 72 h after treatment. These activations, however, were not observed at 24 h after treatment, in contrast to the increase in BDNF and GDNF levels that occurred as early as 6 h after treatment (Figs. 3 and 4). In a preliminary study, we observed that ON-crushing injury upregulated CREB in the retina at 6 h post injury, which then returned to the baseline level within 72 h (not significant, data not shown). Moreover, poloxamer–alginate by itself significantly induced BDNF and GDNF production, albeit to a relatively small extent (Fig. 1). These effects might hinder the specific effects of Leu–Ile in early phases. Poloxamer–alginate also significantly increased ERK activation 48 and 72 h after treatment (Fig. 3). The increases may be attributed to poloxamer 407, the main component of the hydrogel. Although the effects of poloxamer 407 (12,600 Da) on neural tissues are unknown, it has been reported that poloxamer 188 (8400 Da), another tri-block copolymer of ethylene oxide and propylene oxide, repairs cell membrane damage after traumatic brain injury and activates ERK in PC2 cells (a subline-derived from rat pheochromocytoma cell line PC12) (Serbest et al., 2006). It is possible that

poloxamer 407 or its degradation products act on the retinal cell membrane to increase BDNF and GDNF production and consequently activate ERK. Several reports have suggested that activation of ERK and CREB is necessary in the signaling needed to rescue RGCs in ON-axotomized (Choi et al., 2003) or injured retinas (Biermann et al., 2010). BDNF is capable of activating both the ERK pathway (Nakazawa et al., 2002) and CREB, which is induced by ERK (Fujino et al., 2009), in the retina. Although GDNF signaling in retinal protection is not fully understood, it has been shown to activate several ERK pathways in cultured retinal tissues (Hauck et al., 2006). The results of our Western blotting therefore support the hypothesis that Leu–Ile exerts an RGC survival promoting effect via the induction of BDNF and/or GDNF expression. Cen et al. (2006) have additionally reported that Leu–Ile rapidly stimulates both Akt and CREB phosphorylation, which in turn induce GDNF in cultured hippocampal neurons. Therefore, it may be possible that Leu–Ile delays RGC loss without the induction of neurotrophic factors. However, we have previously reported that Leu–Ile attenuated the methamphetamine-induced place preference of mice, while such attenuation by Leu–Ile was not observed in heterozygous knockout (GDNF(+/−)) mice (Niwa et al., 2007). Leu–Ile also inhibited the prolonged immobility time induced by the forced swimming test in mice, while such a reduction in immobility time was not observed in heterozygous knockout (BDNF(+/−)) mice (Furukawa-Hibi et al., 2011). These results suggest that the effects of Leu–Ile depend on BDNF or GDNF expression. This is one possibility that needs to be tested in ON-injured models in the future.

Sustained delivery of neurotrophic factors to the retina is an attractive approach for treating optic neuropathies. Intravitreal injection of biodegradable GDNF microspheres enabled prolonged delivery of GDNF in the retina and rescued RGCs in glaucoma and retinal ischemic models (Jiang et al., 2007; Kyhn et al., 2009). Intravitreal injection of viral vectors encoding neurotrophic factors or of stem cells also results in a prolonged effect on RGC survival in glaucoma and ON-injured models (Schmeer et al., 2002; Martin et al., 2003; Yu et al., 2006). In comparison with these studies, utilization of a hydrogel vehicle for periocular injection cannot offer a sustained delivery of Leu–Ile to the retina; therefore, it may not exert a prolonged effect on RGC survival. It does, however, appear to be a safer approach.

In conclusion, our results indicate that periocular injection of Leu–Ile using *in situ* hydrogels promotes BDNF and GDNF production in the retina and enhances survival of RGCs after ON injury. Leu–Ile may activate ERK and CREB signaling via the induction of these neurotrophic factors. Longer-term periocular delivery of Leu–Ile may be useful for the treatment of RGC degenerative diseases.

Acknowledgments

This project was financially supported by the Collaborative Development of Innovative Seeds program (Potentiality verification stage) of the Japan Science and Technology Agency.

References

Alkam, T., Nitta, A., Furukawa-Hibi, Y., Niwa, M., Mizoguchi, H., Yamada, K., Nabeshima, T., 2010. Oral supplementation with Leu–Ile, a hydrophobic dipeptide, prevents the impairment of memory induced by amyloid beta in mice via restraining the hyperphosphorylation of extracellular signal-regulated kinase. Behav. Brain Res. 210, 184–190.

Biermann, J., Grieshaber, P., Goebel, U., Martin, G., Thanos, S., Di Giovanni, S., Lagrèze, W.A., 2010. Valproic acid-mediated neuroprotection and regeneration in injured retinal ganglion cells. Invest. Ophthalmol. Vis. Sci. 51, 526–534.

Cen, X., Nitta, A., Ohya, S., Zhao, Y., Ozawa, N., Mouri, A., Ibi, D., Wang, L., Suzuki, M., Saito, K., Ito, Y., Kawagoe, T., Noda, Y., Ito, Y., Furukawa, S., Nabeshima, T., 2006. An analog of a dipeptide-like structure of FK506 increases glial cell line-derived neurotrophic factor expression through cAMP response element-binding protein activated by heat shock protein 90/Akt signaling pathway. J. Neurosci. 26, 3335–3344.

Choi, J.S., Kim, J.A., Joo, C.K., 2003. Activation of MAPK and CREB by GM1 induces survival of RGCs in the retina with axotomized nerve. Invest. Ophthalmol. Vis. Sci. 44, 1747–1752.

Dahlmann-Noor, A.H., Vijay, S., Limb, G.A., Khaw, P.T., 2010. Strategies for optic nerve rescue and regeneration in glaucoma and other optic neuropathies. Drug Discov. Today 15, 287–299.

Dean, D.O., Kent, C.R., Tytell, M., 1999. Constitutive and inducible heat shock protein 70 immunoreactivity in the normal rat eye. Invest. Ophthalmol. Vis. Sci. 40, 2952–2962.

Dumortier, G., Grossiord, J.L., Agnely, F., Chaumeil, J.C., 2006. A review of poloxamer 407 pharmaceutical and pharmacological characteristics. Pharm. Res. 23, 2709–2728.

Fujino, H., Kitaoka, Y., Hayashi, Y., Munemasa, Y., Takeda, H., Kumai, T., Kobayashi, S., Ueno, S., 2009. Axonal protection by brain-derived neurotrophic factor associated with CREB phosphorylation in tumor necrosis factor-alpha-induced optic nerve degeneration. Acta Neuropathol. 117, 75–84.

Furukawa-Hibi, Y., Nitta, A., Ikeda, T., Morishita, K., Liu, W., Ibi, D., Alkam, T., Nabeshima, T., Yamada, K., 2011. The hydrophobic dipeptide Leu–Ile inhibits immobility induced by repeated forced swimming via the induction of BDNF. Behav. Brain Res. 220, 271–280.

Hauck, S.M., Kinkl, N., Deeg, C.A., Swiatek-de Lange, M., Schöffmann, S., Ueffing, M., 2006. GDNF family ligands trigger indirect neuroprotective signaling in retinal glial cells. Mol. Cell Biol. 26, 2746–2757.

Jiang, C., Moore, M.J., Zhang, X., Klassen, H., Langer, R., Young, M., 2007. Intravitreal injections of GDNF-loaded biodegradable microspheres are neuroprotective in a rat model of glaucoma. Mol. Vis. 13, 1783–1792.

Karim, M.Z., Sawada, A., Mizuno, K., Kawakami, H., Ishida, K., Yamamoto, T., 2009. Neuroprotective effect of nipradilol [3,4-dihydro-8-(2-hydroxy-3-isopropylamino)-propoxy-3-nitroxy-2H-1-benzopyran] in a rat model of optic nerve degeneration. J. Glaucoma 18, 26–31.

Koeberle, P.D., Ball, A.K., 1998. Effects of GDNF on retinal ganglion cell survival following axotomy. Vision Res. 38, 1505–1515.

Koeberle, P.D., Ball, A.K., 2002. Neurturin enhances the survival of axotomized retinal ganglion cells in vivo: combined effects with glial cell line-derived neurotrophic factor and brain-derived neurotrophic factor. Neuroscience 110, 555–567.

Kyhn, M.V., Klassen, H., Johansson, U.E., Warfvinge, K., Lavik, E., Kiilgaard, J.F., Prause, J.U., Scherfig, E., Young, M., la Cour, M., 2009. Delayed administration of glial cell line-derived neurotrophic factor (GDNF) protects retinal ganglion cells in a pig model of acute retinal ischemia. Exp. Eye Res. 89, 1012–1020.

Lin, H.R., Sung, K.C., Vong, W.J., 2004. *In situ* gelling of alginate/pluronic solutions for ophthalmic delivery of pilocarpine. Biomacromolecules 5, 2358–2365.

Maeda, K., Sawada, A., Matsubara, M., Nakai, Y., Hara, A., Yamamoto, T., 2004. A novel neuroprotectant against retinal ganglion cell damage in a glaucoma model and an optic nerve crush model in the rat. Invest. Ophthalmol. Vis. Sci. 45, 851–856.

Martin, K.R., Quigley, H.A., Zack, D.J., Levkovitch-Verbin, H., Kielczewski, J., Valenta, D., Baumrind, L., Pease, M.E., Klein, R.L., Hauswirth, W.W., 2003. Gene therapy with brain-derived neurotrophic factor as a protection: retinal ganglion cells in a rat glaucoma model. Invest. Ophthalmol. Vis. Sci. 44, 4357–4365.

Nakazawa, T., Tamai, M., Mori, N., 2002. Brain-derived neurotrophic factor prevents axotomized retinal ganglion cell death through MAPK and PI3K signaling pathways. Invest. Ophthalmol. Vis. Sci. 43, 3319–3326.

Nitta, A., Nishioka, H., Fukumitsu, H., Furukawa, Y., Sugiura, H., Shen, L., Furukawa, S., 2004. Hydrophobic dipeptide Leu–Ile protects against neuronal death by inducing brain-derived neurotrophic factor and glial cell line-derived neurotrophic factor synthesis. J. Neurosci. Res. 78, 250–258.

Niwa, M., Nitta, A., Yamada, Y., Nakajima, A., Saito, K., Seishima, M., Shen, L., Noda, Y., Furukawa, S., Nabeshima, T., 2007. An inducer for glial cell line-derived neurotrophic factor and tumor necrosis factor-alpha protects against methamphetamine-induced rewarding effects and sensitization. Biol. Psychiatry 61, 890–901.

Parrilla-Reverter, G., Agudo, M., Sobrado-Calvo, P., Salinas-Navarro, M., Villegas-Pérez, M.P., Vidal-Sanz, M., 2009. Effects of different neurotrophic factors on the survival of retinal ganglion cells after a complete intraorbital nerve crush injury: a quantitative in vivo study. Exp. Eye Res. 15, 32–41.

Rieke, E.R., Amaral, J., Becerra, S.P., Lutz, R.J., 2010. Sustained subconjunctival protein delivery using a thermosetting gel delivery system. J. Ocul. Pharmacol. Ther. 26, 55–64.

Schmeer, C., Straten, G., Kügler, S., Gravel, C., Bähr, M., Isenmann, S., 2002. Dose-dependent rescue of axotomized rat retinal ganglion cells by adenovirus-mediated expression of glial cell-line derived neurotrophic factor in vivo. Eur. J. Neurosci. 15, 637–643.

Serbest, G., Horwitz, J., Jost, M., Barbee, K., 2006. Mechanisms of cell death and neuroprotection by poloxamer 188 after mechanical trauma. FASEB J. 20, 308–310.

Tsai, R.K., Chang, C.H., Wang, H.Z., 2008. Neuroprotective effects of recombinant human granulocyte colony-stimulating factor (G-CSF) in neurodegeneration after optic nerve crush in rats. Exp. Eye Res. 87, 242–250.

Vehanen, K., Hornof, M., Urtti, A., Uusitalo, H., 2007. Peribulbar poloxamer for ocular drug delivery. Acta Ophthalmol. 86, 91–96.

Weber, A.J., Viswanáthan, S., Ramanathan, C., Harman, C.D., 2010. Combined application of BDNF to the eye and brain enhances ganglion cell survival and function in the cat after optic nerve injury. Invest. Ophthalmol. Vis. Sci. 51, 327–334.

Wenzel, J.G., Balaji, K.S., Koushik, K., Navarre, C., Duran, S.H., Rahe, C.H., Kompella, U.B., 2002. Pluronic F127 gel formulations of deslorelin and GnRH reduce drug degradation and sustain drug release and effect in cattle. J. Control. Release 85, 51–59.

Yan, Q., Wang, J., Matheson, C.R., Urich, J.L., 1999. Glial cell line-derived neurotrophic factor (GDNF) promotes the survival of axotomized retinal ganglion cells in adult rats: comparison to and combination with brain-derived neurotrophic factor (BDNF). J. Neurobiol. 38, 382–390.

Yu, S., Tanabe, T., Dezawa, M., Ishikawa, H., Yoshimura, N., 2006. Effects of bone marrow stromal cell injection in an experimental glaucoma model. Biochem. Biophys. Res. Commun. 344, 1071–1079.

BRAIN RESEARCH 1419 (2011) 97-104

Available online at www.sciencedirect.com

SciVerse ScienceDirect

www.elsevier.com/locate/brainres

BRAIN RESEARCH

Research Report

Heparin-binding EGF-like growth factor is required for synaptic plasticity and memory formation

Atsushi Oyagi[a], Shigeki Moriguchi[b], Atsumi Nitta[c], Kenta Murata[a], Yasuhisa Oida[a], Kazuhiro Tsuruma[a], Masamitsu Shimazawa[a], Kohji Fukunaga[b], Hideaki Hara[a,]*

[a]*Molecular Pharmacology, Department of Biofunctional Evaluation, Gifu Pharmaceutical University, Gifu 501-1196, Japan*
[b]*Department of Pharmacology, Graduate School of Pharmaceutical Sciences, Tohoku University, Sendai 980-8578, Japan*
[c]*Department of Pharmaceutical Therapy & Neuropharmacology, Faculty of Pharmaceutical Sciences, Graduate School of Medicine and Pharmaceutical Sciences, University of Toyama, Toyama 930-0194, Japan*

ARTICLE INFO

Article history:
Accepted 1 September 2011
Available online 9 September 2011

Keywords:
CaMKII
HB-EGF
LTP
Memory
Neurotrophic factor

ABSTRACT

Heparin-binding epidermal growth factor-like growth factor (HB-EGF), a member of epidermal growth factor (EGF) family, is a potent mitogenic peptide for various types of cells. HB-EGF is widely expressed in central nervous system, including hippocampus and cerebral cortex, and is considered to play pivotal roles in the developing and adult nervous system. In this study, we assessed the role of HB-EGF in learning and memory by testing HB-EGF conditional knock-out mice (KO) in two different learning tasks, and evaluated the long-term potentiation (LTP) in hippocampus slices from these mice. The HB-EGF KO mice were impaired in spatial memory in the Morris water maze and in fear learning in a passive avoidance test. HB-EGF KO mice also showed an impaired LTP, and reduction in activity of Ca^{2+}/calmodulin-dependent protein kinase II (CaMKII) and phosphorylated GluR1. We also found that the levels of neurotrophic factors, such as nerve growth factor (NGF), brain-derived neurotrophic factor (BDNF), neurotrophin-3 (NT-3), or glial cell line-derived neurotrophic factor (GDNF), were altered in several brain regions in the HB-EGF KO mice. These results confirm the importance of the HB-EGF in synaptic plasticity and memory formation.

1. Introduction

Heparin-binding epidermal growth factor-like growth factor (HB-EGF) is a member of the EGF family of growth factors that includes EGF, transforming growth factor (TGF)-α, amphiregulin, betacelulin, and neuregulin (Barnard et al., 1995; Higashiyama et al., 1991; Watanabe et al., 1994). In the central nervous system, HB-EGF is widely distributed in neurons and neuroglia throughout the brain, and is especially enriched in the hippocampus, cerebral cortex, and cerebellum (Mishima et al., 1996). HB-EGF binds to and activates the EGF receptor (EGF receptor/ErbB1) (Higashiyama et al., 1991), ErbB4 (Elenius et al., 1997), and has been implicated in neuronal survival and glial/stem cell proliferation (Farkas and Krieglstein, 2002; Kornblum et al., 1999; Nakagawa et al., 1998). For instance, HB-EGF has been reported to exert protective effects in rodent models of ischemic brain injury (Jin et al., 2004) and to enhance neurogenesis in the subventricular zone and hippocamal dentate gyrus (Jin et al., 2003; Jin et al., 2004). We have also previously reported that ventral forebrain specific HB-EGF knockout (KO) mice show aggravated

* *Corresponding author at:* Molecular Pharmacology, Department of Biofunctional Evaluation, Gifu Pharmaceutical University, 1-25-4 Daigaku-nishi, Gifu 501-1196, Japan. Fax: +81 58 230 8126.
E-mail address: hidehara@gifu-pu.ac.jp (H. Hara).

0006-8993/$ – see front matter © 2011 Elsevier B.V. All rights reserved.
doi:10.1016/j.brainres.2011.09.003

brain injury induced by a middle cerebral artery occlusion (Oyagi et al., 2011).

We have also previously demonstrated that HB-EGF conditional KO mice exhibit several neurobehavioral abnormalities, including impairments of prepulse inhibition, social interaction, and cognitive function, which were accompanied by aberrant cortical spine morphology (Oyagi et al., 2009). These results indicate that HB-EGF may be one of the important contributors to neuronal development and higher brain function.

HB-EGF is widely expressed in the central nervous system, including the hippocampus and cerebral cortex, where it serves in cognitive functions, however, very few studies have yet examined the involvement of HB-EGF in synaptic plasticity and memory formation. In the present study, we assessed the role of HB-EGF in learning and memory by testing HB-EGF conditional KO in two different learning tasks: the Morris water maze and passive avoidance tests. We also measured long-term potentiation (LTP), activation of various protein kinases in hippocampal slices, and neurotrophic factor levels in various regions of HB-EGF KO mice.

2. Results

2.1. *Spatial memory acquisition and retention in the Morris water maze test*

HB-EGF mRNA and immunoreactivity have been localized in hippocampus (Hayase et al., 1998; Oyagi et al., 2009), which is one of the most well characterized regions for spatial memory formation. We first examined spatial memory acquisition and retention abilities in the Morris water maze test to determine the involvement of HB-EGF in hippocampus-dependent memory formation. Both WT and HB-EGF KO mice exhibited similar escape latencies to the hidden platform with daily training (Fig. 1B), suggesting that the learning kinetics of reference memory were similar between each group [genotype; $F_{(1,19)}=1.048$, $P>0.05$, time; $F_{(4,76)}=32.604$, $P<0.01$, genotype×time; $F_{(4,76)}=1.808$, $P>0.05$]. In a probe trial, WT mice spent significantly more time in the target quadrant than in other quadrants, indicating that they remembered the place where the platform used to be (Figs. 1 A and C) [WT; $F_{(3,48)}=44.557$, $P<0.0001$]. In contrast, HB-EGF KO mice spent less time than the WT mice in this area (Fig. 1 C). No significant differences were observed in swim speed between WT and HB-EGF KO mice [WT; 18.4±0.82 cm/s (n=13), KO; 17.6±1.47 cm/s (n=8)].

2.2. *Fear memory in passive avoidance test*

Next, we conducted a passive avoidance test. Passive avoidance conditioning was used to determine whether HB-EGF KO mice exhibited altered abilities in a learning task; in this paradigm, lasting context-fear association can be imparted with a single training session (Duvarci et al., 2005). During the training session, WT and HB-EGF KO mice showed a similar latency in crossing to the dark side of the chamber (Fig. 2A), whereupon they received a single foot shock. When animals were tested at 24 h after conditioning, HB-EGF KO mice exhibited a significantly decreased latency to cross to the foot shock-paired dark side (Fig. 2A).

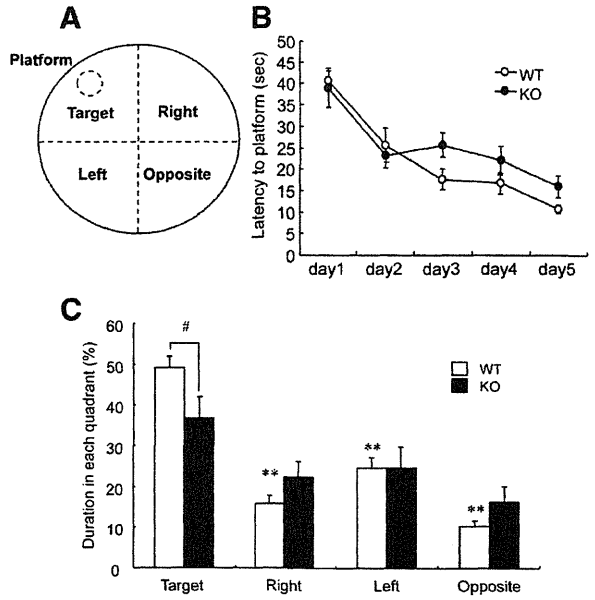

Fig. 1 – Morris water maze test results for HB-EGF KO mice. (A) Diagrammatic illustration shows the positions of the platform and each quadrant. (B) Latency to escape to the hidden platform in WT (n=13) and HB-EGF KO (n=8) mice in the training test. (C) Duration in each quadrant of HB-EGF WT (n=13) and KO (n=8) mice in the probe test. Values are means±SEM. ** $p<0.01$ vs. target quadrant. # $p<0.05$ vs. WT in target quadrant.

Ectodomain shedding of HB-EGF, regulated by ADAMs, is critical for its function. Therefore we evaluated the effect of KB-R7785, which inhibits the activities of ADAMs, on memory formation in the passive avoidance test. During the training session, no significant differences in performance were noted between each group (Fig. 2B). However, on the day of testing, the significantly shorter step-through latencies for entering the dark compartment were seen for the KB-R7785 (100 mg/kg, s.c.) treated mice than for the vehicle-treated mice (Fig. 2B), which implied that the continuous administration of KB-R7785 could inhibit memory retention in mice. Administration of the positive control, scopolamine (3.0 mg/kg, i.p.), resulted in a similar shortening of the latency to enter the dark compartment when compared with the behavior of vehicle-treated mice (Fig. 2B).

2.3. *Long-term potentiation (LTP) in hippocampus CA1 neuron*

Because impaired memory implies abnormal hippocampal plasticity in HB-EGF KO mice, we next analyzed LTP induced by a high-frequency stimulation (HFS) in hippocampus CA1 neurons using slice preparations. In control slices from WT mice hippocampus, HFS (100 Hz, 2 trains) of the Schaffer collateral/commissural pathways induced LTP in the hippocampal CA1 region, which lasted over 60 min (1 min after HFS; 265.7± 23.1% of baseline, 60 min after HFS; 205.0±34.2% of baseline, n=5) (Figs. 3A, B, and C). On the other hand, a marked reduction of LTP was observed in slices from HB-EGF KO mice (1 min after HFS; 143.4±14.6% of baseline, 60 min after HFS; 130.8±16.2% of